REVIEW ARTICLE

Cantilever transducers as a platform for chemical and biological sensors

Nickolay V. Lavrik
Oak Ridge National Laboratory, Oak Ridge, Tennessee 37831-6141

Michael J. Sepaniak
University of Tennessee, Knoxville, Tennessee 37996-1200

Panos G. Datskos[a)]
Oak Ridge National Laboratory, Oak Ridge, Tennessee 37831-6141and University of Tennessee, Knoxville, Tennessee 37996-1200

(Received 24 November 2003; accepted 10 April 2004; published online 21 June 2004)

Since the late 1980s there have been spectacular developments in micromechanical or microelectro-mechanical (MEMS) systems which have enabled the exploration of transduction modes that involve mechanical energy and are based primarily on mechanical phenomena. As a result an innovative family of chemical and biological sensors has emerged. In this article, we discuss sensors with transducers in a form of cantilevers. While MEMS represents a diverse family of designs, devices with simple cantilever configurations are especially attractive as transducers for chemical and biological sensors. The review deals with four important aspects of cantilever transducers: (i) operation principles and models; (ii) microfabrication; (iii) figures of merit; and (iv) applications of cantilever sensors. We also provide a brief analysis of historical predecessors of the modern cantilever sensors. © *2004 American Institute of Physics.* [DOI: 10.1063/1.1763252]

I. INTRODUCTION

A. General definitions and concepts

Concepts of chemical sensors have been a subject of extensive research efforts in recent decades. According to established definitions, a chemical sensor consists of a physical transducer (i.e., a transducer of physical quantities into convenient output signals) and a chemically selective layer (see Fig. 1) so that measurable output signals can be produced in response to chemical stimuli.[1] Specific binding sites present in chemically selective layers provide affinity of targeted analytes to the sensor active area. Highly selective receptor layers can be designed using concepts of molecular and biomolecular recognition [Fig. 1(B)]. It is often the physical transducer that imposes both fundamental and practical limitations on the figures of merit achievable with the respective class of chemical sensors. As a result, implementation of a transduction principle or innovative transducer design is always a significant milestone in the area of chemical sensors.

Until the late 1980s, the main fundamental transduction modes used in chemical sensors could be categorized as[2,3] (a) thermal, (b) mass, (c) electrochemical, and (d) optical. Each of these detection modes is associated with features that are complementary rather than competitive with respect to the other, and a search of an ''ideal transducer'' has continued. During the last two decades, advances in microelectromechanical systems (MEMS) have facilitated development of sensors that involve transduction of mechanical energy and rely heavily on mechanical phenomena.[4–11] Development of microfabricated cantilevers for atomic force microscopy (AFM)[12] signified an important milestone in establishing efficient technological approaches to MEMS sensors. However, the key concepts[13–18] as well as early experimental studies[19–24] related to mechanical transducers for chemical sensors can be traced back far beyond the MEMS era as is accepted today.

Functionality of MEMS sensors is based on mechanical movements and deformations of their micromachined components, such as single-clamped suspended beams (cantilevers), double-clamped suspended beams (''bridges''), or suspended diaphragms. Cantilever structures similar to AFM probes are some of the simplest MEMS that can also be considered as basic building blocks for a variety of more complex MEMS devices. Since the advent of scanning probe microscopy (SPM), the fabrication and characterization of microscale cantilevers useful as AFM probes[12,25] have been a subject of extensive research efforts.[26–28] As a result of more recent advances in several converging areas of science and technology, not only a variety of sophisticated probes became available for SPM but also an innovative family of physical, chemical, and biological sensors based on cantilever technology was shaped out.[6,9–11,29–33] Broader interest in MEMS transducers[4] can be explained by their potential for applications in optical imaging,[34,35] telecommunica-

[a)]Author to whom all correspondence should be addressed; electronic mail: datskospg@ornl.gov

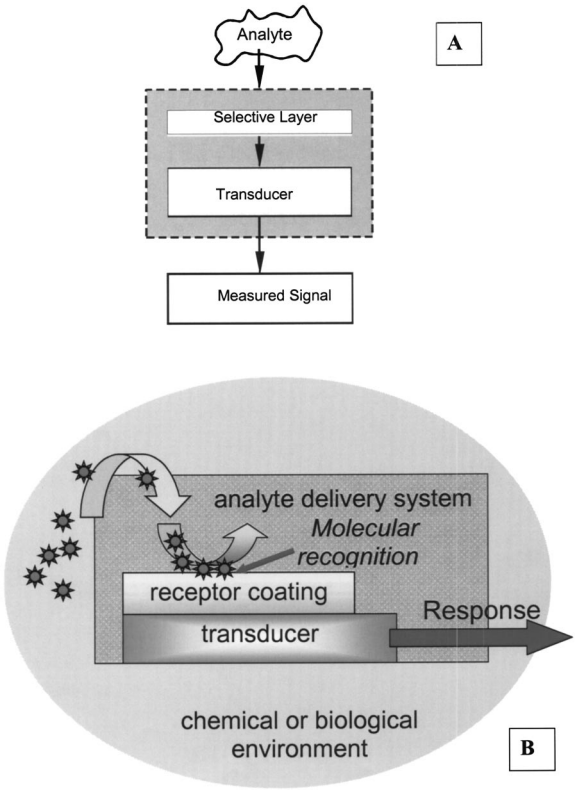

FIG. 1. Generalized structure a chemical sensor. (A) Schematic representation of a chemical sensor that produces an output signal in response to the presence of a target analyte. (B) A chemical sensor with a molecular recognition receptor layer provides a highly selective response.

tions,[36–38] and data storage.[39–44] While MEMS transducers span a great variety of designs,[4] devices with very simple cantilever-type configurations appeared to be especially suitable as transducers of physical, chemical, and biological stimuli into readily measured signals.[29,45] In Figs. 2(A)–2(C), we show examples of different cantilever devices. Figure 2(A) illustrates a comparison between sizes of commercially available AFM cantilevers and a human hair. Designs of cantilever devices vary substantially depending on the desired parameters. For example, the long thin legs of the cantilever shown in Fig. 2(B) improve thermal isolation between the active part of the device and its surrounding.

The general idea behind MEMS sensors is that physical, chemical, or biological stimuli can affect mechanical characteristics of the micromechanical transducer in such a way that the resulting change can be measured using electronic, optical, or other means.[46] In particular, microfabricated cantilevers together with read-out means that are capable of measuring 10^{-12} to 10^{-6} m displacements can operate as detectors of surface stresses,[5,47–53] extremely small mechanical forces,[54–57] charges,[58–62] heat fluxes,[5,63,64] and IR photons.[65–72] As device sizes approach the nanoscale, their mechanical behavior starts resembling vibrational modes of molecules and atoms (Fig. 3). Dimensional scaling of cantilevers is associated with respective scaling of their mass, frequency, and energy content. In the nanomechanical regime, it is possible to attain extremely high fundamental frequencies approaching those of vibrational molecular modes. Ultimately, very small nanomechanical transducers can be envisioned as human-tailored molecules that interact controllably with both their molecular environment and readout components. Nanomechanical resonators with a mass of 2.34×10^{-18} g and a resonance frequency of 115 MHz were fabricated and displacement of $2\times10^{-15}\,\mathrm{m\,Hz^{-1/2}}$ were measured.[73] Mass sensitivity of only a few femtograms was reported recently using nanoscale resonators.[74]

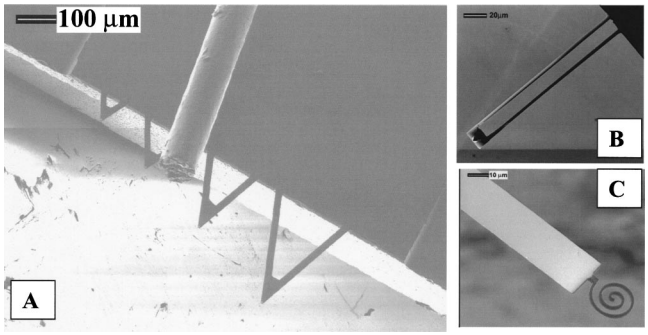

FIG. 2. Examples of cantilever devices. (A) Commercially available cantilevers used in AFM. (B) and (C) Modified rectangular cantilevers with increased thermal isolation are optimized for calorimetric detection.

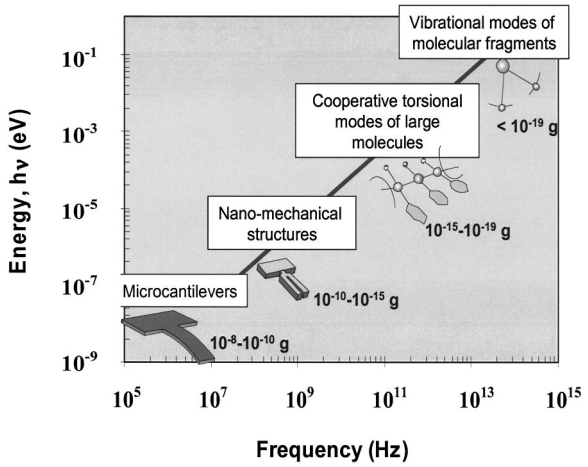

FIG. 3. Cantilevers: Spatial scaling is associated with respective scaling of masses, frequencies, and energies. In the nanomechanical regime, it is possible to attain extremely high fundamental frequencies approaching those of vibrational molecular modes.

This article focuses almost exclusively on MEMS sensors with transducers in a form of cantilevers or analogous structures with more complex shapes and one or several anchoring points. We will use the terms ''cantilever'' and ''bridge'' throughout the text of this section to denote devices analogous to, respectively, single-clamped and double-clamped suspended beams of various sizes and shapes. For simplicity, we will mainly use the term ''MEMS,'' although derived terms, such as microoptoelectromechanical systems, and biological microelectromechanical systems could also be justified in this content to emphasize specific features of certain sensors based on micromechanical transducers. This review is structured largely around the four main aspects relevant to MEMS sensors: (i) operation principles and models; (ii) microfabrication; (iii) figures of merit; and (iv) applications of cantilever sensors. In addition, we also provide a brief historical background on cantilever sensors over a pe-

riod that spans a century. Since many MEMS are truly multifaceted devices that may integrate several transduction modes, a significant part of the article is devoted to principles of their operation.

B. Early devices utilizing direct conversion of chemical stimuli into mechanical responses

Studies of mechanical phenomena associated with changes in the chemical environment have a substantial historical background. In 1924, Palmer[19] studied coherence of loosely contacting thin filaments induced by electromagnetic waves in the presence of different gases and analyzed correlation between the observed responses and the heat of gas absorption. Almost at the same time, Meehan[21] observed adsorption-induced expansion of yellow pine charcoal exposed to carbon dioxide vapors and showed that this was a reversible process. Later, Yates[75] conducted similar studies on the expansion of porous glass exposed to nonpolar gases such as Ar, N_2, O_2, H_2, and Kr. A description of a chemical detector based on a cantilever mechanical transducer can be found in the patent issued to Norton as early as 1943.[14] A further refinement of this principle described by Norton was described by Shaver in 1969.[15]

Mechanical stresses and deformations produced in response to a changing chemical environment have also drawn attention as a principle of powering miniature mechanical devices. For example, in the 1960s, Kuhn[76] and Steinberg *et al.*[17] developed the concept of devices that provide direct conversion of chemical stimuli into mechanical energy.[18,77] Work on such devices referred to as *mechanochemical engines* has not been pursued since then primarily because of the difficulty associated with microfabrication. Furthermore, practical implications of these devices were limited until advances in microtechnology and, more recently, in MEMS opened up an opportunity to fabricate miniaturized mechanical components routinely.

C. Evolution from macro- to micro-mechanical transducers

Long before the advent of AFM, macroscopic cantilever devices and mechanical resonators were used by many researchers as very sensitive transducers and highly precise oscillators. One of the earliest examples is an electronic circuit that provided a precision time standard by using a macroscopic tuning fork.[78] As was already mentioned in the previous section, the use of macroscopic cantilevers in chemical sensors can be traced back to the 1940s;[14] Norton proposed a hydrogen detector based on a macroscopic bimetallic plate. Norton's work was revisited almost three decades later by Shaver[15] who also used large 100 mm long, 125 μm thick bimaterial cantilevers in a hydrogen sensor. A decade later, Taylor and coworkers from Oak Ridge National Laboratory, Oak Ridge, Tennessee studied bending induced by molecular adsorption of He, H_2, NH_3, and H_2S on large nickel cantilevers (100 mm long) coated with 80 nm of gold.[79] The operation of sensors described by Norton and Shaver was based on very high solubility of hydrogen gas in palladium and concomitant expansion of the metal, i.e., the same phenomenon that was used recently in an integrated on-chip MEMS-based hydrogen sensors.[80] Cantilever deflections observed in the studies of Taylor and coworkers were associated with adsorbate-induced stresses (i.e., a surface rather than bulk phenomenon) and indicated another fundamental mechanism[81] that was later utilized in a variety of cantilever-based chemical and biological sensors. Macroscopic cantilever transducers were also demonstrated to be rather sensitive calorimetric devices useful, for instance, as IR detectors. In 1957 Jones used a thin, few millimeter long metallic strip in order to detect IR radiation due to thermal expansion of the strip.[82]

Optical means for measuring mechanical responses of macroscopic mechanical transducers with submicrometer accuracy have existed since the 1920s.[20] However, a simple visual approach to cantilever readout often used in the early studies[14,15,79,82] could not provide the accuracy and the sensitivity required for a macroscale mechanical transducers to constitute practically appealing chemical sensors. Yet another difficulty of using macroscale cantilever transducers for practical applications was their extremely high susceptibility to external vibrations stemming from their large suspended masses and, respectively, low resonance frequencies. Hence, cantilever transducers had attained little practical appeal until both microscopic cantilevers and more precise means for their readout became widely available.

Interestingly, in the 1960s Newell and his coworkers from Westinghouse Research Laboratories, Pittsburgh, PA, developed a device integrating a field effect transistor and a thin micromachined metal plate suspended above its gate.[16] This work by Newell and his coworkers introduced the idea of ''the resonance gate transistor,'' according to which mechanical oscillation of a resonating microcantilever could be converted into an oscillatory electronic signal and amplified by the field effect transistor. In 1967, Newell discussed a generalized concept of electromechanical devices based on ''miniaturized tuning forks'' and reported evaluation of their fundamental parameters.[83,84] While the scope of this work was not related to chemical sensing, it represented a successful implementations of a microfabricated cantilever transducer integrated with an electronic readout. Notably, by creating a density of 500 resonance gate transistors per one-inch silicon wafer,[85] batch fabrication of MEMS devices was demonstrated. Nonetheless, significant technological challenges of microfabricated cantilevers prevented resonant gate transistors from becoming widespread at that time. This, however, was not the case with piezoelectric devices[86] based on bulk[87] and surface acoustic waves which were explored as transducers for chemical sensors[88–90] and drew significant attention in the subsequent decade.[1,91–95] Except for very few studies,[96,97] the idea of microfabricated transducers based on suspended resonating or deformable structures[16,24,83–85,98,99] remained almost abandoned until the advent of AFM.[12]

II. FUNDAMENTAL MODELS

Analogous to contact and tapping modes of AFM,[46] cantilever based sensors also involve measurements of cantilever deflections, resonance frequencies and, in some cases,

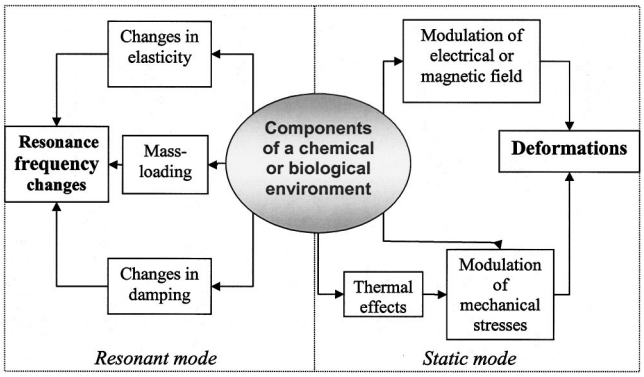

FIG. 4. Conversion of input stimuli into output signals by cantilever transducers is associated with a number of transduction mechanisms. Depending on the measured parameter—structural deformations or resonance frequency changes—the mode of sensor operation can be refereed to as either *static* or *resonant*. Each of these modes, in turn, can be associated with different transduction scenarios.

damping characteristics. However, the mechanisms that translate various components of a physical, chemical, or biological environment into these parameters are generally different from the mechanisms that are operative in AFM. The variety of transduction mechanisms that are involved in the functioning of cantilever sensors is depicted in Fig. 4. Depending on the measured parameter—cantilever deflection or resonance frequency—the mode of cantilever operation can be referred to as either static or dynamic. Each of these modes, in turn, can be associated with different transduction scenarios (Fig. 4). Static cantilever deflections can be caused by either external forces exerted on the cantilever (as in AFM) or intrinsic stresses generated on the cantilever surface or within the cantilever. While cantilever microfabrication technology is capable of producing nearly stress-free suspended beams, additional intrinsic stresses may subsequently originate from thermal expansion, interfacial processes and physicochemical changes. Cantilever sensors operating in the dynamic mode are essentially mechanical oscillators, resonance characteristics of which depend upon the attached mass as well as viscoelastic properties of the medium. For instance, adsorption of analyte molecules on a resonating cantilever results in lowering of its resonance frequency due to the increased suspended mass of the resonator.

Depending on the nature of the input stimuli, microcantilever sensors can be referred to as *physical, chemical, or biological* sensors. The variety of transduction modes (Fig. 4) stems from the fact that a stimulus of each type may affect the mechanical state of the transducer directly or may undergo one or several transformations before the measured mechanical parameter of the transducer is affected. For instance, biochemical interactions can be monitored by detecting IR photons emitted as a result of an exothermic process. In turn, IR photons can be detected by measuring mechanical stresses produced in a MEMS detector as a direct consequence of the photon absorption process.[67] More commonly, however, detection of IR photons by MEMS detectors consists in detecting the temperature increases associated with absorption of IR photon.[68,70,72] Thermal sensitivity of bimaterial cantilevers[13] can also be used to detect molecular and biochemical interfacial interactions due to the heating effects of exothermic reactions or molecular adsorption processes.[5] Alternatively, cantilever transducers can detect chemical and biochemical species more directly due to adsorption-induced stresses[47,49,53,100–103] or mass loading effects.[74,104,105]

Modern MEMS sensors have much in common with their predecessors, such as resonant gate transistors,[16,24,83,84,98,106] acoustomechanical resonance sensors,[92,94,107–110] as well as macroscopic cantilever devices.[13,15,79,111,112] In fact, more than 50 years separated some of the earliest experimental[113] and theoretical[13,114] studies on cantilever systems and the recognition of cantilevers as a platform for chemical sensors by the broader research community.[11,45,64,115–119] Due to this remarkable time span, well-established analytical models of cantilevers are now available and can be used to design and evaluate microcantilever transducers or analogous MEMS for chemical analytical applications. Furthermore, the classical models of cantilever devices have been frequently revisited, refined, and compared against the results of numerical computational methods that become widespread in recent years.[52,120] Nevertheless, simple classical models remain very useful for understanding basic principles of MEMS sensors. Depending on the operation mode of a MEMS sensor, static or dynamic models are applicable.

In the beginning of the 20th century, development of the elasticity theory by Timoshenko[13,114] and experimental studies of thin films by Stoney[113] become major milestones in developing fundamental analytical models that would subsequently find wide applications in MEMS analysis. These classical models[13,113] focused primarily on static deformations of purely elastic beams and plates have been revisited more recently.[8,50–52,121–124] As applied to various cantilever sensors operating in the static mode, the expression for strain-induced deformations of bimaterial plates derived by Timoshenko[13] in the 1920s appeared to be of particular significance.

A. Static deformations

In the absence of external gravitational, magnetic, and electrostatic forces, cantilever deformation is unambiguously related to a gradient of mechanical stress generated in the device. Depending on a particular origin of this stress, analytical models suitable for quantitative analysis of microcantilever responses may or may not be available. For instance, simple models are applicable to thermally induced stresses and concomitant deformations of microcantilevers made of two layered materials with different coefficients of thermal expansion. Theoretical evaluation of bimetal thermostats reported by Timoshenko[13] provided an analytical expression for the radius of curvature of a bimaterial cantilever as a function of a temperature change. This deformation resulting from unequal thermal expansion of each layer has been used extensively as an operation principle of thermostats and often referred to as the bimetallic effect. Taking into account the length of the cantilever l, the respective defection of the tip $\Delta z[=l^2/(2R)]$ can be expressed as

$$\Delta z = \frac{3l^2}{t_1+t_2}\left[\frac{\left(1+\frac{t_1}{t_2}\right)^2}{3\left(1+\frac{t_1}{t_2}\right)^2+\left(1+\frac{t_1E_1}{t_2E_2}\right)\left(\frac{t_1^2}{t_2^2}+\frac{t_2E_2}{t_1E_1}\right)}\right] \times(\alpha_1-\alpha_2)\Delta T, \quad (1)$$

where t_1 and t_2 is the thickness of the two layers of the bimaterial plate, E_1 and E_2 are the Young's moduli, and α_1, and α_2 are the thermal expansion coefficients for the materials of these layers, respectively. While the objective of Timoshenko's original work was evaluation of bimaterial thermostats, a strain induced deformation is also an important response mechanism of cantilever based chemical sensors in which a chemically selective layer undergoes expansion upon interaction with its chemical medium.[124]

More recently, various modifications of Eq. (1) have been used to predict thermally induced deflections of microscopic bimaterial cantilevers.[8,63] In order to evaluate calorimetric sensitivity of a bimaterial cantilever, Barnes *et al.*[63] combined Eq. (1) with the expression for a thermal flux along the cantilever and found that the deflection of the cantilever tip Δz is given by

$$\Delta z = \frac{5}{4}(\alpha_1-\alpha_2)\frac{t_1+t_2}{t_2^2K}\frac{l^3}{\lambda_1t_1+\lambda_2t_2}P,$$
$$K = 4+6\left(\frac{t_1}{t_2}\right)+4\left(\frac{t_1}{t_2}\right)^2+\frac{E_1}{E_2}\left(\frac{t_1}{t_2}\right)^3+\frac{E_2}{E_1}\left(\frac{t_1}{t_2}\right), \quad (2)$$

where λ_1 and λ_1 are the thermal conductivities of the two layers and P is the absorbed power.

Femto-Joule level calorimetric sensitivity of conventional AFM cantilevers demonstrated experimentally by Barnes *et al.* is consistent with the theoretical predictions made using Eq. (2).[63] As applied to chemical and biological sensors, cantilever based calorimetry enables two transduction scenarios (Fig. 4). First, the presence of analyte species can be detected due to the heat associated with their adsorption on the transducer. Second, the heat produced in the course of a subsequent chemical reaction on the cantilever surface can be characteristic of the analyte presence. However, molecular adsorption processes and interfacial chemical reactions may also affect mechanical stresses in thin plates more directly and independently of the thermal effects. Apart from fundamental interest in the direct conversion of chemical energy into mechanical energy,[18,76] this mechanism means that cantilever transducers are compatible with many responsive phases and can function in both gas and liquid environments.

It has been known since the 1960s that molecular and atomic adsorbates on atomically pure faces of single crystals tend to induce significant surface stress changes. Long before the first microfabricated cantilevers were created, changes in surface stresses in these systems had been studied by measuring minute deformations of relatively thin (up to 1 mm) plates. Using this method, often referred to as the beam-bending technique,[49,111,112] Kosch *et al.* studied[125,126] surface stress changes induced by adsorption of atoms on atomically pure surfaces in vacuum. Using the Shuttleworth equation,[81] the surface stress σ and surface free energy γ can be interrelated

$$\sigma = \gamma+\left(\frac{\partial\gamma}{\partial\epsilon}\right), \quad (3)$$

where σ is the surface stress. The surface strain $d\epsilon$ is defined as the relative change in surface area $\partial\epsilon=\partial A/A$. In many cases, the contribution from the surface strain term can be neglected and the free energy change approximately equals the change in surface stress.

Adsorbate and chemically induced surface stresses have also been extensively studied with regard to their role in colloidal systems. Important examples of colloidal phenomena associated with the surface stress changes include swelling of hydrogels upon hydration or formation of surfactant monolayers at the air-water interface.[127] Fundamental studies of adsorption- and absorption-induced mechanical phenomena, however, had limited implications for chemical sensors until mass produced AFM microcantilevers became widely available. As compared with their macroscopic predecessors, microcantilevers coupled with the optical lever readout greatly simplified real-time measurements of surface stress changes in the low $\mathrm{mN\,m^{-1}}$ range.

Cantilevers intended for use as chemical sensors are typically modified so that one of the sides is relatively passive while the other side exhibits high affinity to the targeted analyte. In order to understand how different modifying coatings provide responses of cantilever sensors in the static bending mode, it is useful to consider the three distinctive models. The first model is most adequate when interactions between the cantilever and its environment are predominantly surface phenomena. Adsorption of analyte species on transducer surfaces may involve physisorption (weak bonding, binding energy <0.1 eV) or chemisorption (stronger bonding, binding energy >0.3 eV). Physisorption is associated with van der Waals interactions between the adsorbate and the adsorbent substrate. As the analyte species approach the surface, they can polarize the surface creating induced dipoles. The resulting interactions are associated with binding energies less than 0.1 eV. Much higher binding energies are characteristic of chemical bonding between the analyte and the surface in the case of chemisorption.

In general, changes in surface stresses can be largely attributed to changes in Gibbs free energy associated with adsorption processes. An example of this situation is given in Fig. 5, where chemisorption of straight-chain thiol molecules on a gold coated cantilever is schematically depicted. Since spontaneous adsorption processes are driven by an excess of the interfacial free energy, they are typically accompanied by the reduction of the interfacial stress. In other words, surfaces usually tend to expand (see Fig. 5) as a result of adsorptive processes. This type of surface stress change is defined as compressive, referring to a possibility of return of the surface into the original compressed state. The larger the initial surface free energy of the substrate, the greater the possible change in surface stress results from spontaneous adsorption processes. Compressive surface stresses were ex-

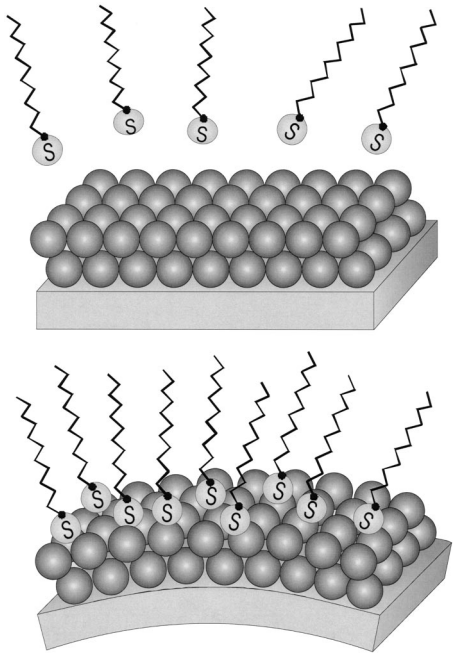

FIG. 5. Schematic depiction of chemisorption of straight-chain thiol molecules on a gold coated cantilever. Spontaneous adsorption processes are driven by an excess in the interfacial free energy, and accompanied by reduction of the interfacial stress.

perimentally observed on the gold side of gold coated cantilevers exposed to vapor-phase alkanethiols.[102,103]

In many cases, adsorbate-induced deformations of thin plates can be accurately predicted using a modification of the relationships originally derived by Stoney and von Preissig[113,121]

$$\frac{1}{R}=\frac{6(1-\upsilon)}{Et^2}\Delta\sigma, \tag{4}$$

where R is the radius of microcantilever curvature, υ and E are Poisson's ratio and Young's modulus for the substrate, respectively, t is the thickness of the cantilever, and $\delta\sigma$ is the differential surface stress. Knowledge of the radius of curvature R allows the tip displacement of a microcantilever with length l tip to be determined by

$$\Delta z=\frac{1}{2}\frac{l^2}{R}=\frac{3l^2(1-\upsilon)}{Et^2}\Delta\sigma. \tag{5}$$

When adsorbate-induced stresses are generated on ideal smooth surfaces or within coatings that are very thin in comparison to the cantilever, the analysis according to Eq. (3) is rather straightforward. Using Eq. (4) or (5), the predictions for the cantilever bending can be based on the expected surface stress change. Alternatively, responses of cantilever sensors converted into surface stress changes can be analyzed as the measure of the coating efficiency independently of the transducer geometry.

The second model of analyte-induced stresses (Fig. 6) is applicable for a cantilever modified with a much thicker than a monolayer analyte-permeable coating.[128,129] Taking into account interactions of the analyte molecules with the bulk of the responsive phase, a predominant mechanism of cantilever deflection can be described as deformation due to analyte-induced swelling of the coating (Fig. 6). Such swelling processes can be quantified using approaches developed in colloidal and polymer science, i.e., by evaluating molecular forces acting in the coating and between the coating and the analyte species. In general, dispersion, electrostatic, steric, osmotic, and solvation forces,[127] acting within the coating can be altered by absorbed analytes. Depending on whether it is more appropriate to describe the responsive phase as solid or gel-like, these altered forces can be put into accordance with, respectively, stress or pressure changes inside the coating. An in-plane component of this change multiplied by the coating thickness yields an apparent surface stress change that can be used in Stoney's model [Eq. (4)] in order to estimate deflections of a cantilever coated with thin, soft, responsive films. It is important to note that the magnitude of apparent surface stress scales up in proportion with the thickness of the responsive phase.

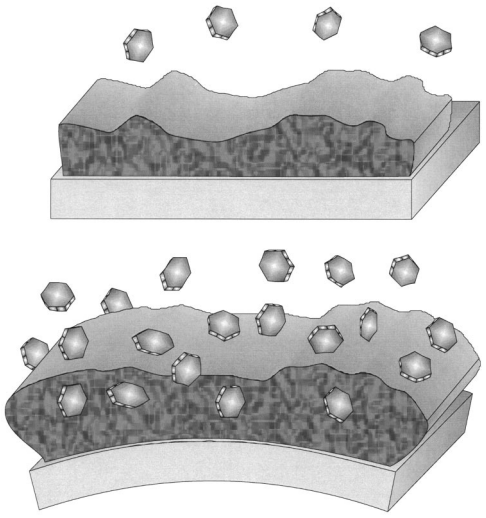

FIG. 6. Schematic depiction of analyte-induced cantilever deformation when the surface is modified with a thicker analyte-permeable coating. Interactions of the analyte molecules with the bulk of the responsive phase lead to coating swelling and can be evaluated using approaches employed in colloidal and polymer science.

The third model (Fig. 7) is most relevant to nanostructured interfaces and coatings, such as surface-immobilized colloids, that have been recently recognized as a very promising class of chemically responsive phases for cantilever sensors and actuators.[74,130–134] It is worthy to note that grain boundaries, voids, and impurities have been long known as being responsible for high intrinsic stresses in disordered, amorphous, and polycrystalline films.[125]

Analyte-induced deflections of cantilevers with structured phases (Fig. 7) combine mechanisms of bulk, surface, and intersurface interactions.[127] A combination of these mechanisms facilitates efficient conversion of the energy of receptor-analyte interactions into mechanical energy of cantilever bending. Recent studies demonstrated that up to two orders of magnitude increases in cantilever responses can be obtained when receptor molecules are immobilized on nanostructured instead of smooth gold surfaces.[133,135,136] Furthermore, nanostructured responsive phases offer an approach to substantially increase the number of binding sites per canti-

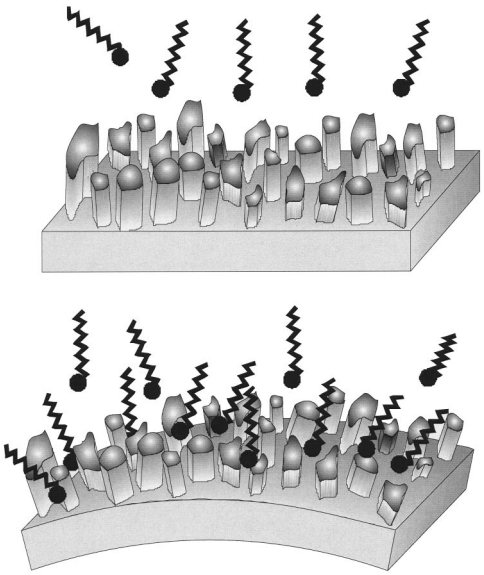

FIG. 7. Schematic depiction of analyte-induced cantilever deformation in the case of a structured modifying phase. Analyte-induced deflections of cantilevers with structured phases combine mechanisms of bulk, surface, and intersurface interactions.

lever without compromising their accessibility for the analyte. In fact, many of these nanostructured phases exhibit behaviors of *molecular sponges*. Although deflections of cantilevers with nanostructured coatings or thicker hydrogel layers cannot be accurately predicted using the analytical models mentioned above, estimates for the upper limit of the mechanical energy produced by any cantilever transducer can always be based on simple energy conservation. This upper limit in available energy is given by the product of the energy associated with the binding site-analyte interaction and the number of such interactions on the cantilever surface.

B. Resonance operation

Cantilever transducers operating in gases or in vacuum can be treated as weakly damped mechanical oscillators. Their resonant behavior can be readily observed using excitation in alternated electric, electromagnetic, or acoustic fields. Furthermore, minute sizes and mass of microfabricated cantilevers makes them susceptible to thermally induced noise, which has the same origin as Brownian motion of small particles in liquids. Therefore, cantilever sensors may operate in the resonant mode either with or without external excitation.

As a first approximation, it can be assumed that the cantilever tip displacement is directly proportional to the force exerted on the cantilever tip. Then, a simplified model of a resonating cantilever transducer can be based on the Hook's law applied to a rectangular leaf spring with an effective suspended mass m_0 and a spring constant k. The effective suspended mass of a cantilever can be related to the total mass of the suspended portion of the beam m_b through the relationship: $m_0 = n\, m_b$, where n is a geometric parameter. For a rectangular cantilever, n has a typical value of 0.24 and the spring constant k is given by[46]

$$k = \frac{E w t^3}{4 l^3}, \tag{6}$$

where E is the modulus of elasticity for the material composing the cantilever and w, t, l are the width, thickness, and length of the cantilever, respectively. Assuming a spring constant k and an effective suspended mass m_0, which consists of both a concentrated and a distributed mass, the microcantilever fundamental resonance frequency f_0 in the absence of damping can be approximated as[46]

$$f_0 = \frac{1}{2\pi} \sqrt{\frac{k}{m_0}}. \tag{7}$$

Equation (7) is often used as a starting point in estimating the mass sensitivity of resonating cantilever sensors of various shapes and sizes.[74,104,105,115,137,138] As a rule, Eq. (7) gives a good approximation of the resonance frequency for a weakly damped mechanical resonator, such as a microscopic cantilever in air. However, more accurate calculations of the microcantilever resonance frequencies require the dissipation of the resonator energy through various mechanisms to be taken into account. This can be done by introducing a mechanical quality factor (Q-factor). In the case of damping force being proportional to the cantilever velocity (viscous damping), the resonance frequency of the mechanical resonator is[46,139]

$$f_{0,Q} = \frac{1}{2^{3/2}\pi} \sqrt{\frac{k}{m_0}} \frac{\sqrt{2Q-1}}{Q}. \tag{8}$$

When Eqs. (7) and (8) are used to analyze gravimetric responses of resonating microcantilever transducers, it is reasonable to assume that the spring constant k remains unaffected. However, there is some evidence that chemical and physical interactions between a cantilever transducer and its environment do affect the cantilever spring constant thus making analysis of gravimetric responses less straightforward.[115,140,141] For instance, appreciable changes in the cantilever spring constant were reported in response to varying ionic strength of an aqueous NaCl solution. In particular, spring constant of an AFM cantilever was reported to change by over one order of magnitude from 0.5×10^{-3} to 7.5×10^{-3} N/m as the NaCl concentration increased from 0.05 to 0.8 M/L.[141] In another study by the same group, a model of a tout string was used in order to relate changes in the spring constant and adsorbate-induced surface stresses.[142] This evaluation led to the following relationship:

$$\Delta k = \frac{\pi^2}{4 n_1} (\Delta s_1 + \Delta s_2), \tag{9}$$

where Δs_1 and Δs_2 are the changes in the surface stress on the top and bottom surface of the microcantilever (before and after the adsorption of analytes), $n = 0.24$ for a rectangular microcantilever, and n_1 is another geometrical factor. While a spring constant change of 0.38 N/m was calculated for a gold coated AFM cantilever as a result of its exposure to a thiol,[142] applicability of the tout spring model to microcantilever transducers and Eq. (9) is questionable. Unfortunately, more appropriate models that could explain effects of the chemical environment on the microcantilever stiffness are

still lacking. When the damping effect of the medium is rather strong, both resonance frequency shifts and the *Q*-factor can be related to changes in the viscosity of the medium. Such a dependency was experimentally observed using standard AFM cantilevers placed in different gases[143] or water-glycerol mixtures.[144]

In summary, the resonant operation of cantilever transducers encompasses three mechanisms: (i) adsorbate-induced mass-loading; (ii) chemically induced changes in the cantilever stiffness; and (iii) mechanical damping by the viscous medium. A more detailed discussion of various damping mechanisms in microcantilever transducers related to external as well as intrinsic dissipation phenomena is given in the next section.

C. Energy dissipation in microcantilevers

Mechanical deformations in MEMS always involve appreciable dissipation of mechanical energy into thermal energy. Mechanisms that determine this dissipation are related to inelastic phenomena in solids and viscous properties of fluids.[145] In analogy to other types of resonators, the quality factor (or *Q*-factor) is commonly used to quantify energy dissipation in MEMS. The *Q*-factor is inversely proportional to the damping coefficient[146] or total energy lost per cycle of vibration in a microcantilever transducer and can be defined as

$$Q = \frac{2\pi W_0}{\Delta W}, \tag{10}$$

where W_0 and ΔW_0 are, respectively, the mechanical energy accumulated and dissipated in the device per vibration cycle.

It is important to emphasize that both the resonance behavior of any microcantilever and its off-resonance thermal noise are critically dependent on the *Q*-factor.[69,146–151] Therefore, the *Q*-factor is one of the important characteristic of MEMS sensors operating in both resonance and static regimes. Based on the spectral analysis, the *Q*-factor can be calculated as a ratio of the resonance frequency f_0 to the width of the resonance peak at its half amplitude. Hence, the *Q*-factor is frequently used to characterize the degree of the resonance peak sharpness. Alternatively, *Q*-factors of mechanical oscillators can be related to time constants of exponentially decaying oscillator amplitude during a ring-down process[150]

$$Q = \pi \tau_d f_0, \tag{11}$$

where τ_d is the time constant of the exponentially decaying ring-down amplitude.

The *Q*-factor of microcantilevers depends on a number of parameters, such as cantilever material, geometrical shape, and the viscosity of the medium. Obviously, increased damping of a microcantilever oscillator by the medium translates into lower *Q*-factor values[143] as compared to the same oscillator in vacuum. Models of drag forces exerted on solid bodies in fluids[145,152,153] can be used to evaluate viscous damping effects. A very important distinctive feature of viscous damping is that the damping force is proportional to the linear velocity of the vibrating cantilever. The other damping mechanisms, involving clamping loss and internal friction within the microcantilever, were reviewed in recent studies by Yasumura *et al.*[150] As a rule, these dissipation mechanisms are associated with damping forces independent of the linear cantilever velocity. Clamping loss has an insignificant contribution to the total dissipation in the case of longer microcantilever with high length-to-width and width-to-thickness ratios. However, ultimate minimization of clamping loss can be achieved in oscillators with double-paddle or ''butterfly'' geometries[154] rather than single-clamped cantilevers or double-clamped bridges. Hence, fundamental studies of intrinsic friction effects in MEMS often rely on measurements of resonances in double-paddle resonators. *Q*-factors as high as 10^5 were reported for torsional butterfly-shaped resonators fabricated from a single-crystal silicon.[155–157]

Internal friction can be linked to a variety of physical phenomena, in particular, thermoelastic dissipation (TED)[152] motion of lattice defects, phonon-phonon scattering, and surface effects.[158,159] The TED limit and phonon-phonon scattering mechanisms correspond to very high *Q*-factors (10^6 to 10^8), which can hardly be observed experimentally due to the contribution from other dissipation mechanisms present in real MEMS. The fact that surface effects may limit *Q*-factors of MEMS oscillators in vacuum can be verified by annealing the device and controllably changing its surface.[150] As the thickness of the oscillator decreases, TED becomes even a less significant mechanism of dissipation.[150]

As mentioned previously *Q*-factors of MEMS resonators in vacuum can be very high.[157,160] However, *Q*-factors of rectangular microcantilevers in air are typically in the range of 10 to 1000 while cantilever transducers in aqueous solutions rarely have *Q*-factors above 10. Very strong viscous damping in liquids makes resonant operation of microcantilevers, and, in turn, measurements of adsorbed mass using microcantilever sensors, rather challenging. In order to overcome the difficulties of resonant cantilever operation in liquids, cantilever transducers can be used as a part of a self-oscillating system with a positive feedback.[46,161] For instance, the signal from the microcantilever readout can be amplified and fed back to a piezoelectric actuator connected to the microcantilever. Such a self-oscillating system can be described by an apparent quality factor Q' defined as increased in the mean square of the cantilever deflections[162]

$$Q' = \frac{\langle z_{\mathrm{dr}}^2 \rangle}{\langle z_{\mathrm{th}}^2 \rangle} Q. \tag{12}$$

It was reported that the positive feedback scheme applied to cantilevers in water results in apparent *Q*-factors Q' that exceed the intrinsic *Q*-factors by two to three orders of magnitude.[161] Taking into account the apparent *Q*-factor, expression for the cantilever response function $|G(f)|^2$ (or $|G(\omega)|^2$) can be rewritten as[162]

$$|G(\omega)|^2 = \frac{\dfrac{1}{m_0^2}}{(\omega_0^2 - \omega)^2 + \left(\dfrac{\omega_0 \omega}{Q'}\right)^2}. \tag{13}$$

While it may be convenient to use an apparent Q-factor Q' in order to describe the spectral response of the self-oscillating system, the intrinsic thermal noise $\Psi_{th}(\omega)$ is always a function of an intrinsic Q-factor[162] as discussed later.

III. MICROFABRICATION

Microfabrication of MEMS has been a subject of extensive research and development efforts over the past 25 years. The relevant microfabrication processes have been described in great detail in literature.[4,163–167] In general, fabrication of MEMS devices is based on two distinct micromachining strategies: (i) bulk micromachining and (ii) surface micromachining. Bulk micromachining involve removal of substantial portions (i.e., ''bulk'') of the substrate. Bulk micromachining is often used to create devices with three-dimensional (3D) architecture or suspended structures. Surface micromachining remain the original substrate mostly intact and use it as a base for a device formed as a result of additive (deposition) and subtractive (etching) processes.[4]

Although a variety of substrates and thin films can be used to fabricate microcantilever devices using bulk or surface micromachining, one of the most preferred substrates is single crystal silicon. In fact, MEMS fabrication relies heavily on approaches previously developed for microfabrication of conventional electronic devices. Silicon oxide, silicon nitride, polycrystalline silicon (polysilicon), and metal films are some of the most common films used in surface micromachining of both MEMS[168] and more traditional microelectronic devices. As applied to microcantilever fabrication, low pressure chemical vapor deposition (LPCVD) and plasma-enhanced chemical vapor deposition (PECVD) techniques are widely used to form silicon dioxide and silicon nitride structural or sacrificial layers.[4]

Typically, fabrication of suspended microstructures, such as a cantilever transducer, consists of deposition, patterning, and etching steps that define, respectively, thickness, lateral sizes, and the surrounding of the cantilever. One of the frequently used approaches in microcantilever fabrication involves deposition of a sacrificial layer on a prepatterned substrate followed by deposition of a structural material layer (such as a silicon nitride layer or a polysilicon layer) using an LPCVD or PECVD processes. By varying the conditions of these deposition processes, the stress and stress gradient in the deposited layers can be minimized so that suspended structures do not exhibit significant deformation after they are released by etching of the sacrificial layer. The cantilever shapes can be defined by patterning the silicon nitride film on the top surface using photolithography followed by reactive ion etching (RIE). Photolithographic patterning of the structural material (silicon nitride or polysilicon) on the bottom surface is used to define mask for anisotropic bulk etch of Si. The silicon substrate is then etched away to produce free-standing cantilevers. Using a similar sequence of processes, single crystal silicon cantilevers can be created with the difference that doping of silicon or epitaxy of a doped silicon layer substitutes deposition of a silicon nitride layer (the p-doped silicon plays a role of an etch stop layer).[116,169]

In order to avoid any bulk micromachining, such as through-etch of silicon in KOH, various cantilever fabrication processes based on the use of a sacrificial layer were developed.[116,169,170] These processes frequently rely on silicon oxide as a material for the sacrificial layer.[166,170] The use of a sacrificial layer for fabrication of silicon nitride membranes, bridges, and cantilevers is illustrated in Fig. 8. While the use of a sacrificial layer introduces additional restrictions on the material choice, it enables process flows that are fully compatible with standard complementary-metal-oxide-semiconductor (CMOS) chip technology.[117,171–173]

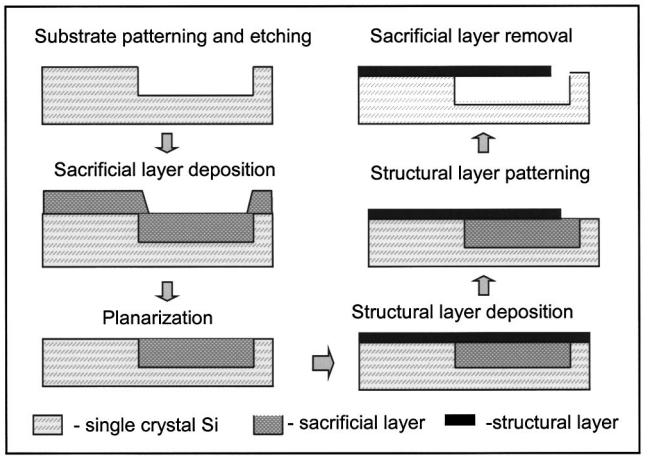

FIG. 8. Illustration of the steps in a process flow used for fabrication of silicon nitride membranes, bridges, and cantilevers. The process involves a deposition of a structural silicon nitride layer on a silicon wafer with a prepatterned sacrificial layer. The cantilever shapes can be defined by patterning the silicon nitride film on the top surface using photolithography followed by reactive RIE.

Specialized MEMS transducers can be rapidly prototyped by using standard rectangular cantilevers as a starting material and using focused ion beam (FIB) for their structural modification.[74] Figure 9 shows two examples of cantilever thermal detectors optimized for calorimetric spectroscopy applications that were fabricated by applying FIB milling to a 500 μm long and 100 μm wide commercially available cantilevers. The improved calorimetric performance of the detector shown in Fig. 9 is due to a substantially narrowed (only 1 μm wide) region that connects the suspended cantilevered structure and the base and provides a very low thermal conductance.

Details of cantilevers design and fabrication are largely defined by the mode of the sensor operation, readout methods, and specific applications. A 50 to 150 nm metal layer deposited on the top side of cantilever detectors provides reflectivity required for the optical readout. Readouts using charge or tunneling effects also require parts of the transducer to be metallized.[60,174,175] In the case of MEMS thermal detectors based on the bimaterial effect, more complex configurations of cantilever transducers may be preferable.[170,176] Metal layers with a high coefficient of thermal expansion deposited on silicon or silicon nitride cantilevers are essential for bimaterial regions in order to achieve high responsivity of MEMS thermal detectors. Piezoelectric and piezoresistive[177] readout methods require one of the cantilever layers or a coating on the cantilever to be made out of a piezoelectric or piezoresistive material.

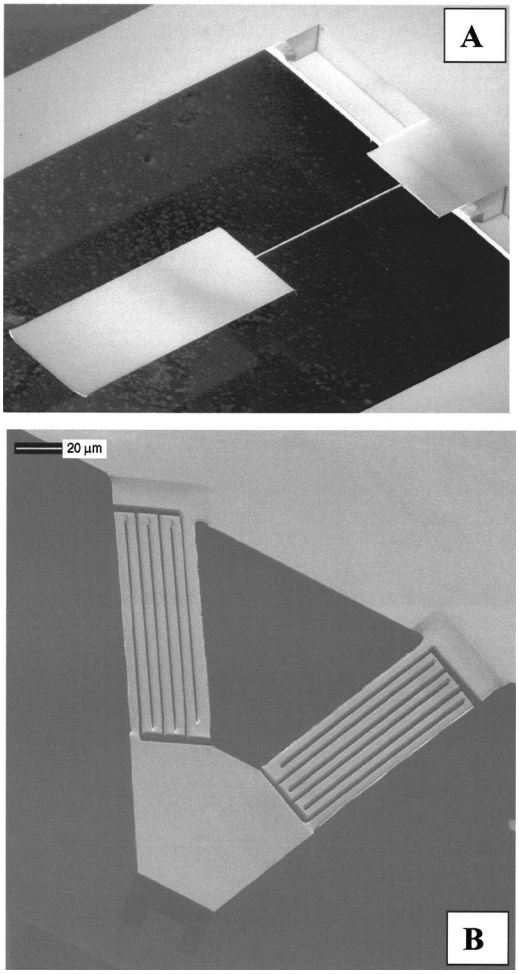

FIG. 9. Example of silicon cantilevers modified using FIB milling. The increased path-length or the narrowed region connecting the suspended rectangular structure to the base provides substantially smaller thermal conductance as compared to the unmodified cantilever.

Commercially available AFM probes made of silicon or silicon nitride have been used extensively in research on cantilever based sensors.[6,10,11,29–33,178] In fact, main structural and geometrical requirements to cantilever transducers for sensor applications are similar to those applicable in AFM. In analogy to AFM cantilevers (Fig. 2), cantilever transducers for MEMS sensors are usually fabricated from silicon or silicon nitride and have typical thicknesses in the range of 0.5 to 5 μm. The typical lengths of cantilevers for both AFM and sensor applications are in the range of 100 to 500 μm and approximately correspond to spring constants of, respectively, 1 to 0.01 $\mathrm{N\,m^{-1}}$. Fabrication of AFM probes is based on well-established process flows that provide low cost, high yield, and good reproducibility of the resulting devices. However, AFM cantilevers are designed and fabricated to satisfy a number of the application-specific requirements, which become partly redundant in the case of cantilever transducers for sensor applications. The most obvious of such redundant features is the presence of a sharp tip on the cantilever end and the accessibility of the tip for a sample surface. Therefore, fabrication of cantilever sensors can even be simplified in comparison to fabrication of AFM probes. This does not, however, take into account the fact that a practical MEMS sensor should ultimately integrate a cantilever transducer, its readout, and an interface with the environment.

In the case of chemical and biological sensors, noble metal coatings provide surfaces that can be selectively modified with synthetic or biological receptors using thiol-gold reaction schemes.[100,101,135,179,180] It was found that palladium and gold coatings can be used in MEMS sensors in order to achieve chemical specificity to hydrogen gas and mercury vapor, respectively.[115,124] Polymeric and macromolecular compounds in a form of 5 nm to 5 μm thick films were shown to provide sensitivity to various organic compounds in a vapors phase[117,119,128,180] as well as organic compounds[136] and ionic species in water.[181–183]

IV. COMMON READOUT SCHEMES

Operation of any cantilever sensor relies on real-time measurements of cantilever deflections with at least nanometer accuracy. Therefore, an important part of any cantilever sensor is a readout system capable of monitoring changes in one of the parameters directly related to the cantilever deflection. Such parameters include cantilever tip position, spatial orientation, radius of curvature, and intrinsic stress. Specific requirements for the readout of cantilever sensors can be dictated by the operation mode (either static or dynamic), cantilever design, and materials used as well as the magnitude of expected responses. In this section, we discuss means of cantilever readout that can be broadly classified as optical and electrical.[46] Using optical, piezoresistive, piezoelectric, capacitance, or electron tunneling methods,[46] deformations and resonance frequency shifts of cantilever transducers can be measured with sufficient precision. All these methods are compatible with array formats.

In order to insure the best possible performance of cantilever sensors, inherent advantages and disadvantages of different readout techniques were analyzed in recent studies. The optical beam deflection method was shown to have excellent readout efficiency in the case of cantilevers with a reflecting area of at least a 10×10 $\mu\mathrm{m}^2$. Optical readout techniques may, however, be inefficient when applied to nanocantilevers. The shortcomings of some optical techniques, in particular the optical deflection method, are related to loss of intensity and directionality of optical beams reflected (scattered) by nanosize cantilevers. By contrast, electron transfer methods can be used with cantilevers that are only a few hundred nanometers long. An important issue still to be addressed is the readout of nanocantilevers arranged in dense arrays. Among already explored readout methods, a charge shuttling method is well suited for nanocantilevers arrays. The basic concept of this method is similar to electrostatic charge shuttling demonstrated by Tuominen *et al.*[184] However, implementation of electron transfer signal transduction in aqueous environments is challenging. Electroactive ions in electrolytes tend to cause parasitic currents that overwhelm electron transfer signal. These leakage currents, however, can be significantly reduced by using proper insulation, reducing bias voltage, and controlling electroactive ions in the solution.

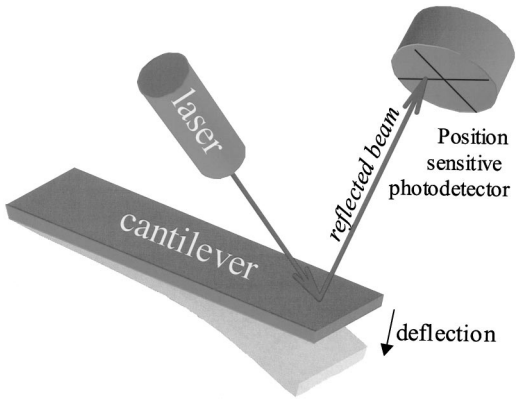

FIG. 10. The "optical lever" readout commonly used to measure deflections of microfabricated cantilever probes in AFM.

A. Optical methods

It is noteworthy that cantilever sensors inherited not only the unique advantages of a microfabricated AFM probe, but also the elegant "optical lever" readout scheme commonly used in modern AFM instruments. Optical methods most extensively used for measurements of cantilever deflections in AFM (Refs. 185–189) include optical beam deflection (also referred to as the "optical lever" method)[186] and optical interferometry.[185,187] In optical beam deflection technique, a laser diode is focused at the free end of the cantilever. The optical lever method proposed for the use in AFM by Meyer and Amer[186] appeared to be simpler and at least as sensitive as more complex interferometric schemes. In the Meyer and Amer studies,[186] a small mirror was attached to a cantilever (made then out of a tungsten wire) so that a position of a laser beam bounced off this mirror could be monitored using a position sensitive photodetector (PSD). This particular optical detection scheme (Fig. 10) can discern extremely small changes in the cantilever bending; measurements of 10^{-14} m displacements were reported. A most common type of PSD is based on a quadrant photodiode that consists of four cells: A, B, C, and D. Each of the cells is coupled to the input of a separate transimpedance amplifier the output voltages of which, V_A, V_B, V_C, and V_D, are proportional to the illumination of the respective quadrant. The normalized differential output, $V_{out}=[(V_A+V_C)-(V_B+V_D)/(V_A+V_B+V_C+V_D)]$, depends linearly on the vertical displacement of the weighted center of the light spot projected by the cantilever. The absence of electrical connections to the cantilever, linear response, simplicity, and reliability are important advantages of the optical lever method. As this method has been used in the vast majority of the work on cantilever sensors, its limitations are well recognized. For instance, changes in the optical properties of the medium surrounding the cantilever may interfere with the output signal. This interference can largely be avoided by using a proper orientation of the cantilever relative to the optical components as discussed in the recent paper of the authors.[136] The effect of the refractive index change as well as other interfering factors can be further suppressed by using differential pairs or arrays of cantilevers. However, applications of cantilever sensors with the optical lever readout are limited to analysis of low opacity, low turbidity media. Another limitation of the optical lever method is related to the bandwidth of PSDs, which typically on the order of several hundred kilohertz.

As the requirements of the high bandwidth become more critical in the case of smaller and stiffer cantilevers that operate in the resonant mode, alternatives to the optical lever readout were explored. For instance, motion of a microscopic structure, such as a cantilever, illuminated with a tightly focused laser beam, produces a change in the spatial distribution of the reflected and/or scattered light. A simple spot photodetector alone or in combination with a knife-edge obstacle can be used to monitor these intensity fluctuations.[190] The readout bandwidth of this method can be extended into the gigahertz range by using a small area, high-speed avalanche photodiode. Approaches based on a single photodetector and light scattering, however, suffer from the interference with ambient light, nonlinear response, and a poorly controllable optical gain. More accurate high-bandwidth optical measurements of cantilever deflections can be carried out using interferometric schemes. Notably, interferometry is an optical technique used for measurements of cantilever deflections in AFM. Interferometry was revisited as a MEMS readout and characterization tool more recently because of its potential for high-bandwidth high-resolution mapping of nanometer scale motions of small cantilevers[56,185] arranged in large 2D arrays. Notably, Rugar *et al.*[55,185] used interferometry to measure subnanometer deflections of the ultrasensitive cantilevers designed for ultrasensitive force measurements that could ultimately permit single-spin magnetic resonance microscopy.

More recently, optical detection techniques were developed independently by a number of groups[70,72] for readout of large arrays of cantilevers motivated by applications of bimaterial cantilevers to uncooled infrared imaging. In those works a single visible laser source illuminates the whole array and the reflected light is either interferometricaly coupled with a reference beam and detected by a charge-coupled device (CCD) imager or directly reflected onto a CCD. These techniques can easily be applied to large two-dimensional arrays limited only by the availability of large size CCD or CMOS visible imagers.

B. Piezoresistance method

Piezoresistivity is the phenomenon of changes in the bulk resistivity with applied stress. When a silicon cantilever with an appropriately shaped doped region is deformed, the change in the resistance of the doped region reflects the degree of the deformation. One of the most common materials that exhibit a strong piezoresistive effects is doped single crystal silicon.[65,177,191,192] However, doped polysilicon cantilever were also fabricated that exhibited excellent piezoresistivity.[117,193] The variation in resistance is typically measured by including the cantilever into a dc-biased Wheatstone bridge. Typical resistance of a silicon microcantilever with a boron doped channel is a few kiloohms. When voltage V is applied to the Wheatstone bridge with resistors of identical initial resistance R, the differential voltage across the bridge can be expressed as $\Delta V=V(\Delta R/4R)$. Piezoresis-

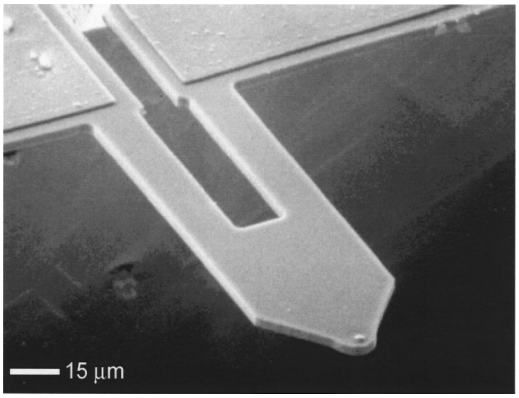

FIG. 11. Example of a piezoresistive cantilever that can be used in both AFM and cantilever sensors.

tive cantilevers are usually designed to have two identical ''legs,'' so that the resistance of the boron channel can be measured by wiring two conductive paths to the cantilever base next to the legs (see Fig. 11). The cantilever shown in Fig. 11 is a commercially available piezoresistive cantilever used in AFM. The disadvantage of the piezoresistive technique is that it requires current to flow through the cantilever. This results in additional dissipation of heat and associated thermal drifts. When the cantilever is heated appreciably above the ambient temperature, any changes in the thermal conductivity of the environment will result in fluctuations of the cantilever temperature that, in turn, may lead to parasitic cantilever deflection and piezoresistance changes.

C. Piezoelectric method

Piezoelectric readout technique requires deposition of piezoelectric material, such as ZnO, on the cantilever. Due to a piezoelectric effect, transient charges are induced in the piezoelectric layer when a cantilever is deformed.[7,194–196]

Lee and White[197] successfully micromachined self-excited piezoelectric cantilevers with resonances in the acoustic frequency range. The piezoelectric cantilever used in these studies had a zinc oxide (ZnO) piezoelectric thin film sandwiched between two aluminum layers on a supporting layer of silicon nitride. A few years later, Lee *et al.*[198] micromachined piezoelectric cantilevers using PZT films. More recently, Adams *et al.*[199] demonstrated a microcantilever chemical detection platform based on an array of piezoelectric microcantilevers with a power consumption in the nanowatts range. Lee *et al.*[198] reported that micromachined piezoelectric cantilevers 100 μm wide, 200 μm long, and 2.1 μm thick had a gravimetric sensitivity of 300 cm^2/g, which enabled detection of 5 ng mass. Characterization of the gravimetric sensitivities in this study was conducted by depositing known amount of gold on the backside of the cantilevers.

The main disadvantage of the piezoelectric as well as piezoresistance readout is that they require electrical connections to the cantilever. An additional disadvantage of the piezoelectric technique is that in order to obtain large output signals it requires the thickness of the piezoelectric film to be well above the values that correspond to optimal mechanical characteristics. Furthermore, the piezoelectric readout is inefficient when slowly changing cantilever deflections need to be measured. Because of the aforementioned disadvantages, application of piezoelectric readout to MEMS sensors is somewhat limited.

D. Capacitance method

Capacitance readout is based on measuring the capacitance between a conductor on the cantilever and another fixed conductor on the substrate that is separated from the cantilever by a small gap.[68,118,200] Changes in the gap due to cantilever deformation result in changes in the capacitance between two conductor plates. Since the capacitance of a flat capacitor is inversely proportional to the separation distance, sensitivity of this method relies on a very small gap between the cantilever and the substrate. Capacitance readout suffers from interference with variations in the dielectric constant of the medium.[201] While differential schemes may eliminate this interference, electrically conductive media, such as electrolytes, make capacitance readout more challenging. One of the main advantages of capacitance readout is that it can be used in integrated MEMS devices that are fully compliant with standard CMOS technology. An interesting variation of the capacitance methods is the ''electron shuttling'' regime that is especially promising for nano-electro-mechanical systems. For instance, Erbe and Blick and Erbe *et al.* reported on the ''quantum bell''[174,175] that consists of five metal-coated cantilever structures and operates in the radio frequency range.

E. Electron tunneling

Electron tunneling has been utilized to measure the deflection of cantilevers in AFM.[12] The electron tunneling occurs between a conducting tip and the cantilever separated by a subnanometer gap. By applying a bias voltage between the tunneling tip and the cantilever causes a flow of electrons between the tip and the cantilever. The tunneling current is very sensitive to the gap and therefore positional changes of the cantilever. This current can be described as[202,203]

$$I \propto V e^{-a\sqrt{\Phi} s}, \tag{14}$$

where V is the bias voltage, Φ is the height of the tunneling barrier, s is the tunneling gap distance, and a is a conversion factor with a value of 1.025 $Å^{-1}\,eV^{-1/2}$. For typical values of Φ and s, the tunneling current increases by one order of magnitude for each 0.1 nm change in s.[202] Therefore, the tunneling readout combines very high sensitivity to relative positional changes, nonlinear response, and a limited dynamic range. Using an electron tunneling readout technique, cantilever displacements as small as 10^{-4} nm have been measured.[202] It is worthy to note that tunneling processes are sensitive to the nature of materials between which the tunneling process occurs, which often translated into challenging requirements to device implementation. Despite its well-known limitations, electron tunneling readout was successfully used in accelerometers,[202] infrared sensors,[204] and magnetic field sensors.[205]

V. FIGURES OF MERIT AND FUNDAMENTAL LIMITATIONS

Some of the most important figures of merit of any chemical or biological sensor are responsivity, limit of detection (LOD), specificity, and reproducibility. As discussed in one of the previous sections, chemical specificity of MEMS sensors may rely on the use of certain responsive phases, such as polymers, self-assembled monolayers, or biological receptors that exhibit higher affinity to the targeted analytes. This reliance on the selective properties of responsive coatings is a common feature of microcantilever sensors operating in both static and resonant regimes. However, transduction efficiency of the two regimes is dictated by very distinct models and mechanisms. Transduction efficiency of the static mode increases when the stiffness of the cantilever is reduced. Therefore, longer cantilevers with very small spring constants are preferable for the use in the static mode. On the other hand, the sensitivity of the resonant mode increases progressively with the operation frequency. As a rule, static and resonant operation of the same microcantilever sensor is characterized by the same specificity but different responsivities and LODs. The fundamental limits of microcantilever chemical transducers are determined by ratios of their responsivities to the levels of intrinsic noise. The next two sections focus on the models specific to optimization of microcantilever sensors based on, respectively, measurements of resonance frequency variations and adsorption-induced deformations. In particular, noise sources that influence the smallest detectable displacements and resonance frequency shifts are discussed.

A. Responsivity of the resonance-based transducers

Although adsorption-induced stresses were extensively explored as a transduction principle in many cantilever sensors, the advantage of the resonant operation is that it can potentially provide mass detection at the single molecule level. The resonance frequency of a cantilever beam depends on its geometry as well as the elastic modulus and density of its material. By changing cantilever dimensions, its resonance frequency can be varied from hundreds of hertz to a few gigahertz (see Fig. 3). For a given cantilevers mass, higher spring constants correspond to higher resonance frequencies. For a given cantilever thickness, shorter cantilevers have higher spring constants. Depending on the cantilever material, gigahertz resonance frequencies can be achieved, when the cantilever length is less than a few microns.[73] Very short cantilevers with high resonance frequency are, therefore, promising in extending the detection limit down to a few molecules.

The dependence of the fundamental frequency on the cantilever parameters for a rectangular cantilever with dimension l, w, and t, respectively, in length, width, and thickness can be expressed as[46]

$$f_0 = \frac{1}{2\pi}\sqrt{\frac{Ewt^3}{4l^3(m_c + 0.24wtl\rho)}}, \tag{15}$$

where ρ is the density of the cantilever material m_c is the concentrated mass. The mass of the adsorbed material can be determined from the initial and final resonance frequency and the initial mass of the cantilever[206]

$$\frac{f_0^2 - f_1^2}{f_0^2} \approx \frac{\Delta m}{m} \quad \text{or} \quad \frac{f_0 - f_1}{f_0} \approx \frac{1}{2}\frac{\Delta m}{m}, \tag{16}$$

where f_0 and f_1 are the initial and final frequency, respectively, and Δm and m are adsorbed mass and initial mass of the cantilever, respectively. If the adsorption is not confined to the very end of the cantilever,[104] Eq. (16) should be modified in order to take into account the effective mass of the cantilever. For any geometry of a microcantilever sensor, the mass responsivity can be defined as

$$S_m = \lim_{\Delta m \to 0} \frac{1}{f_0}\frac{\Delta f}{\Delta \Gamma} = \frac{1}{f_0}\frac{df}{d\Gamma}, \tag{17}$$

where $\Delta\Gamma$ is normalized per active area of the device ($\Delta\Gamma = \Delta m/A$, where A is the active area of the cantilever). Equation (16) shows that the mass responsivity is the fractional change of the resonant frequency of the structure with addition of mass to the sensor. Using Eq. (17), the mass responsivity of a resonating microcantilever sensor can be expressed as[104]

$$S_m = \frac{1}{\rho t}\frac{df}{f_0}, \tag{18}$$

where ρ and t are the density and the thickness of the adsorbate, respectively. Note that the responsivity of a cantilever sensor S_m can be calculated when adsorbate thickness and density are known. It is however, important to emphasize that S_m alone can not be used to evaluate the smallest mass detectable.

Another very important figure of merit of a cantilever sensor is the smallest detectable mass and respective surface density. From Eqs. (17) and (18), the smallest detectable surface density of the adsorbate can be defined as

$$\Delta\Gamma_{\min} = \frac{1}{S_m}\frac{\Delta f_{\min}}{f}, \tag{19}$$

where $\Delta\Gamma_{\min}$ and $\Delta f_{\min}$ are the minimum detectable surface density and minimum detectable frequency change, respectively. In principle, the smallest total detectable mass can be predicted by knowing the detector active area, and the minimum detectable surface density. The estimate for the remaining unknown parameter $\Delta f_{\min}$ can be found taking into account intrinsic noise mechanisms that limit ultimate stability of the resonance frequency. These noise mechanisms are discussed later in this section.

B. Responsivity in the static deformation regime

Adsorption-induced cantilever bending enabled some of the most sensitive detection of trace-level analytes in gases and is a preferable mode of cantilever operation in liquids. A distinctive feature of microcantilever sensors operating in the static mode is that they convert a sum of weak intermolecular forces involved in analyte-sensor interactions into readily measured displacements. This means, that the sensor may respond differently to the same amount of different analytes

depending on the sensor-analyte affinity. Furthermore, adsorbate-induced stresses and associated deformations can be distinguished from the bulk effects, such as changes in volume of thicker polymer films, which also lead to cantilever deformations. Currently, rigorous quantitative evaluation of the sensor responsivity according to these mechanisms is lacking. Semiquantitative analysis of the static mode responsivity can be based on Eqs. (1)–(4) as reported in the literature.[47,124,135,147] In particular, a linear relationship between the cantilever tip displacement and the differential surface stress is given by Eq. (4). According to Eq. (4), there is a quadratic dependency of surface stress induced deflections on the microcantilever length. It is worthy to note that a quadratic dependency of microcantilever deflection responses on the microcantilever length is also predicted by Eq. (1) for the case of bulk interactions. For microcantilever operating in the static mode, an increased length is, therefore, a prerequisite of high responsivity. This conclusion is consistent with the fact that microcantilevers 400 to 1500 μm long were successfully used in chemical sensors operating in the static mode.[133,135,207] Equations (1) and (4) also indicate a strong effect of the thickness of a microcantilever on its deflection responses. In the case of very thin responsive phases or purely surface interactions, Eqs. (1) and (4) predict deflection responses to be inversely proportional to the total thickness of the microcantilever. However, more complex dependencies follow from Eq. (1) in the case of responsive coatings with the thicknesses comparable to the cantilever thickness.

C. Intrinsic noise sources

Noise processes in microcantilever sensors can be divided into processes intrinsic to the device and those related to interactions with its environment (for instance, adsorption-desorption noise) or originated from the readout. Here we focus on the intrinsic noise mechanisms since they determine ultimate fundamental limits of the microcantilever sensors performance. One of the essential features of microcantilevers is that they are mechanical devices (oscillators) that can accumulate and store mechanical energy. Over the past decades there have been extensive efforts to identify the fundamental intrinsic sources of noise in mechanical systems and identify the relationships between parameters of the mechanical system and its noise level.[148]

When a microcantilever detector is equilibrated with the ambient thermal environment (a thermal bath), there is a continuous exchange of the mechanical energy accumulated in the device and thermal energy of the environment. This exchange dictated by the fluctuation dissipation theorem results in spontaneous oscillation of the microcantilever so that the average mechanical energy per mode of cantilever oscillation is defined by thermal energy $k_B T$. Sarid[46] referred to this type of noise as ''thermally induced lever noise.'' In other words, any cantilever in equilibrium with its thermal environment has a ''built-in'' source of white thermal noise $\Psi_{\mathrm{th}}(f)$ given by[162]

$$\Psi_{\mathrm{th}} = \frac{4 m_0 k_B T}{Q}. \tag{20}$$

At frequencies well below the resonance, the amplitude of the resulting thermally induced oscillation of a cantilever beam is proportional to the square root of the thermal energy and can be expressed as

$$\langle \delta z^2 \rangle^{1/2} = \sqrt{\frac{2 k_B T B}{\pi k f_0 Q}}, \tag{21}$$

where k_B is the Boltzmann constant (1.38×10^{-23} J/K), T is the absolute temperature (300 K at room temperature), B is the bandwidth of measurement. As it follows from Eq. (21), lower cantilever stiffness corresponds to higher amplitudes of thermal noise. It should be emphasized, that an intrinsic Q-factor should always be used in Eq. (21).

As a result of the dynamic exchange between cantilever mechanical energy and the ambient thermal energy, the actual frequency f of thermally induced cantilever oscillations at any given moment can noticeably deviate from the resonance frequency f_0. The amplitude of such frequency fluctuations δf_0, due to the exchange between mechanical and thermal energy is[162]

$$\delta f_0 = \frac{1}{z_{\max}} \sqrt{\frac{2 \pi f_0 k_B T B}{k Q}}, \tag{22}$$

where $z_{\max}$ is the amplitude of the cantilever oscillations. Equation (22) predicts increased absolute fluctuations of the resonance frequency δf_0 as the resonance frequency f_0 increases. However, relative frequency instability $\delta f_0 / f_0$ decreases in the case of higher frequency oscillators

$$\frac{\delta f_0}{f_0} = \frac{1}{z_{\max}} \sqrt{\frac{2 \pi k_B T B}{k Q f_0}}. \tag{23}$$

Although Eqs. (21) and (23) are valid for thermally excited cantilevers, they can also be used to evaluate effects of thermal noise on the frequency instability of any externally driven cantilever.[162] As applied to cantilever sensors operating in the resonance mode, an important implication of Eqs. (22) and (23) is that frequency instability due to effects of thermal noise can be minimized by driving the transducer with the highest possible amplitude. In the case of self-oscillating systems with a positive feedback, however, an intrinsic Q-factor should always be used in Eq. (21) since the amplitude of cantilever oscillation $z_{\max}$ is already explicitly taken into account in this analysis.

By changing the physical dimension of a cantilever, its mass detection limit can be affected by many orders of magnitude. For a given cantilever design, the smallest (thermal noise limited) detectable change in the surface density can be found by combining Eqs. (7) and (23)

$$\Delta m_{\mathrm{th}} = 8 \sqrt{\frac{2 \pi^5 k k_B T B}{f_0^5 Q}}. \tag{24}$$

The minimum detectable mass Δm_{th} can then be expressed as

$$\Delta m_{th} = \frac{8 G}{\langle z_{\mathrm{th}}^2 \rangle^{1/2}} \frac{m_0^{5/4}}{k^{3/4}} \sqrt{\frac{k_B T B}{Q}}, \tag{25}$$

where k_B is the Boltzmann constant, T is the temperature of the cantilever, B is the bandwidth of the measurement, k is the cantilever force constant, Q is the mechanical quality factor, m_0 is the initial cantilever mass and $\langle z_{\text{th}}^2 \rangle^{1/2}$ is the root mean square amplitude of the cantilever motion.

Thermomechanical noise of microcantilevers is also known to be a fundamental noise source in AFM.[46,147] Similar analysis is applicable to microcantilever sensors operating in the static regime. The analysis provided by Sarid[46] involves the Q-factor of a vibrating microcantilever, its resonance frequency, ω_0 and stiffness, k. While Q-factor can be defined empirically as the ratio of the resonance frequency to the resonance peak width, knowing the exact mechanisms of cantilever damping is important for evaluation of the thermomechanical noise spectrum. The model evaluated by Sarid[46] assumes that damping of the cantilever is of a viscous nature. Assumption of predominantly viscous damping is valid for microcantilevers in air or water and, therefore, justified for micromechanical devices used as force probes in SPM. In the case of a cantilever in a viscous medium, such as air or water, the damping force is proportional to the cantilever linear velocity. The resulting noise density spectrum can be expressed as[146]

$$\langle \delta z_{\text{TM}}^2 \rangle^{1/2} = \sqrt{\frac{4k_B TB}{Qk} \frac{\omega_0^3}{[(\omega_0^2 - \omega^2)^2 + \omega^2 \omega_0^2 / Q^2]}}. \quad (26)$$

The expression given by Eq. (26) predicts a frequency independent noise density for the frequencies well below the mechanical resonance frequency, ω_0, (i.e., $\omega \ll \omega_0$). At these low frequencies, the rms of the cantilever tip displacement due to thermo-mechanical noise is

$$\langle \delta z_{\text{TM}}^2 \rangle^{1/2} = \sqrt{\frac{4k_B TB}{Qk\omega_0}}. \quad (27)$$

However, at the resonance (i.e., $\omega = \omega_0$)[46]

$$\langle \delta z_{TM}^2 \rangle^{1/2} = \sqrt{\frac{4k_B TBQ}{k\omega_0}}. \quad (28)$$

As follows from Eq. (26), the density of thermomechanical noise follows a $1/f^{1/2}$ dependence below the resonance [see Fig. (12)] when the damping is due to intrinsic friction processes. Analysis of Eqs. (27) and (28) shows that, regardless of the dissipation mechanism, the off-resonance thermomechanical noise is lower in the case of microcantilevers with higher Q-factor and higher k. It should be emphasized that, while predictions based on Eq. (26) are often reported in the literature,[149,208] the noise density calculated according to the two alternative models may substantially deviate from each other at low frequencies.[146,209,210] Furthermore, the intrinsic friction model predicts the low frequency noise to be independent of the cantilever resonance frequency provided that the stiffness k is constant. By contrast, the viscous damping model predicts that the low frequency noise of a microcantilever detector can be decreased by increasing its resonance frequency even without changes in its stiffness. Therefore, knowing the actual mechanisms of mechanical dissipation in the microcantilever detector can be critical in analyzing thermomechanical noise of microcantilever sensors.

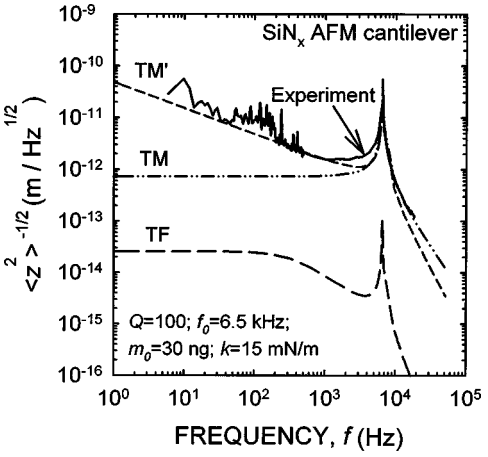

FIG. 12. The contribution of thermomechanical and temperature fluctuation noise to the frequency dependent $\langle \delta z^2 \rangle^{1/2}$. Theoretical plots calculated for a 600 nm thick silicon nitride AFM cantilever coated with 50 nm of gold are shown along with the actual experimental data obtained for this cantilever. The cantilever had a mass of 30 ng, a spring constant of 0.015 N/m, a Q-factor of 100, and a resonance frequency of 6.5 KHz.

In the case of layered (for instance bimaterial) microcantilever transducers an additional noise source needs to be considered. This noise mechanism is related to the temperature sensitivity of bimaterial cantilevers[13,64,114] and the fact that local temperature undergoes appreciable fluctuation at the microscopic scale. As discussed previously by Kruse,[211] the mean square magnitude of these temperature fluctuations is

$$\langle \delta T^2 \rangle = \frac{k_B T^2}{C}, \quad (29)$$

where k_B is Boltzmann's constant, T is the absolute temperature, and C is the total heat capacity of the microcantilever. The temperature fluctuation $\langle \delta T^2 \rangle$ of Eq. (29) is the integration over all frequencies f, where $f = \omega/2\pi$. The spectral density of the root mean square (rms) temperature fluctuations is given by[211]

$$\langle \delta T^2 \rangle^{1/2} = \frac{2\sqrt{k_B B} T}{G^{1/2}\sqrt{1+\omega^2\tau^2}}, \quad (30)$$

where B is the measurements bandwidth and G is the thermal conductance of the principal heat loss mechanism.

Temperature fluctuation noise of the cantilever detector manifests itself as a fluctuation in z and exhibits a frequency dependence influenced by both the thermal response and the mechanical response of the microcantilever. The spontaneous fluctuations in displacement of the microcantilever caused by temperature fluctuations are given by

$$\langle \delta z_{\text{TF}}^2 \rangle^{1/2} = \frac{T\sqrt{4k_B B}}{G^{1/2}\sqrt{1+\omega^2\tau^2}} \frac{1}{\sqrt{\left(1 - \frac{\omega^2}{\omega_0^2}\right)^2 + \frac{\omega^2}{\omega_0^2 Q^2}}}, \quad (31)$$

where ω_0 is resonance frequency of the microcantilever with a quality factor Q. Figure 12 illustrates, the frequency dependence of $\langle \delta z^2 \rangle^{1/2}$ for both thermomechanical and tempera-

ture fluctuation noise and compares these theoretical dependencies with the experimentally measured noise behavior of a standard silicon nitride AFM cantilever.

VI. DEMONSTRATED APPLICATIONS OF CANTILEVER SENSORS

A. Gas phase analytes

Detection of mercury vapors reported by Thundat *et al.*[115] was one of the first gas sensor applications of microscopic cantilevers. Commercially available delta-shaped silicon nitride AFM cantilevers [Ultralevers, Park Scientific, Sunnyvale, CA, see Fig. 2(A)] were used in those studies. The typical length, thickness, and force constant of these cantilevers were, respectively, 180 μm, 0.6 μm, and 0.06 N/m. An evaporated 50 nm gold coating provided affinity of one side of the cantilevers to mercury. The measurements of static deflections and resonance frequencies were based on the Multi-Mode Nanoscope III AFM head (Digital Instruments, Santa Barbara, CA) which provided the optical lever readout of the cantilevers. It was found that both resonance frequencies and static deflections of the gold coated cantilevers underwent changes in presence of mercury vapor (30 $\mu g\,m^{-3}$) added to a nitrogen carrier gas. When one side of the cantilevers was completely coated with gold, the resonance frequency of the cantilevers increased as a result of exposure to mercury vapors. This rather unexpected result was explained by competing effects of the absorbed mercury on the cantilever force constant and on the cantilever suspended mass. It was concluded that interaction of mercury with the gold coating led to a lowering of the cantilever resonance frequency as a result of a relatively small increase in the cantilever effective mass and a more significant increase in the cantilever force constant. This model was confirmed by the fact that exposure to mercury vapors did lower the resonance frequency when only an end portion of the cantilever was coated with gold. In the latter experiment, the region close to the clamping point (which largely defines the cantilever force constant) remained without gold and, therefore, was unaffected in presence of mercury.

Ferrari and coworkers[7] used ceramic cantilevers actuated by piezoelectric excitation to measure resonant frequency changes due to adsorption of water. Ferrari *et al.*[7] used poly(N-vinylpyrrolidinone) and poly(ethyleneglycol) as hydrophilic coating materials and obtained frequency shifts of about 500 and 1400 Hz for relative humidity changes from 12% to 85%, respectively.

Dual (static/dynamic) mode responses of gold coated cantilevers were reported for several other gaseous phase analytes, in particular, 2-mercaptoethanol.[138] In the case of 2-mercaptoethanol, analyte-induced deflections rather than changes in the resonance frequency of gold-coated AFM cantilevers was found to be a preferable mode of sensor operation. Measurements of cantilever deflections permitted detection of mercaptoethanol vapor at concentrations down to 50 part per billion (ppb). The calibration curve obtained in the static deflection mode had a slope of 0.432 nm per ppb in the concentration range of 0–400 ppb.

Fairly high sensitivity and selectivity demonstrated in the early studies on cantilever sensors relied on properties of some metals used as active coatings. For instance, gold is a very chemically inert metal that, nevertheless has very high reactivity toward mercaptans (or thiols), i.e., compounds with one or more sulfohydryl (-SH) groups. High solubility of hydrogen in palladium and palladium based alloys is another mechanism that leads to selective interaction of metal coatings with gas-phase analytes. Good sensitivity of Au and Pd coated cantilevers to, respectively, mercury and hydrogen was subsequently used to implement a palm-sized, self-contained sensor module with spread-spectrum-telemetry reporting.[118] The device utilized polysilicon cantilevers operating in the static deflection mode and integrated with CMOS circuitry that provided their capacitive read-out as well as radio-frequency output for telemetry. The implemented prototype provided reversible, real-time hydrogen sensing and dosimetric (cumulative) mercury-vapor sensing. It was shown in a separate study[212] that a dosimetric mode of hydrogen sensing can also be realized using cantilevers transducers. For this purpose, alpha platinum oxide was used as a coating that undergoes reduction and, therefore, irreversible mass loss in presence of hydrogen. Commercially available AFM cantilevers were coated with 20–50 nm platinum oxide films using reactive sputtering of platinum. Exposure of the sensor to 4% hydrogen in argon resulted in both static cantilever and resonance frequency changes. These changes reached saturation in about 30 min, thus indicating complete reduction of platinum oxide. Overall changes in the coating mass were estimated to be less than a nanogram. In addition to steady the state responses associated with irreversible chemical and physical changes in the coating, the observed transient features in the bending response were consistent with the expected thermal response due to the exothermic oxidation of hydrogen.

As inorganic coatings alone cannot provide the selectivity patterns sought in many applications, modification of cantilevers with chemically selective organic layers has been a subject of more recent studies. One of the first cantilever sensors with organic coatings was a humidity sensor described by Thundat *et al.*[144] In those studies, silicon nitride AFM cantilevers were coated with gelatine, by contacting one side of the cantilever with a 0.1% gelatine solution in distilled water. The deposited gelatine solution was dried by placing the cantilever in the desiccator for two days. When the thus prepared cantilever was exposed to atmosphere of gradually increased humidity, both cantilever deflections and increases in the resonance frequency were observed. The sensor sensitivity measured in the static deflection mode was very high, which even somewhat limited the dynamic range of this sensor [0%–60% relative humidty (R.H.)]. The calibration slope reported for the resonance mode was 55 Hz per % R.H. Another design of a cantilever humidity sensor employed cantilevers with integrated piezoresistive readout.[117] The design included both humidity sensitive and reference cantilevers as a part of a Wheatstone bridge. The layered silicon/silicon oxide cantilevers were 200 μm long, 50 μm wide, 1.5 μm thick with deflection sensitivity $z^{-1}\,(\Delta R/R)$ of approximately $10^{-6}\,nm^{-1}$. Using a glass capillary and a mi-

cromanipulator, the active (humidity sensitive) cantilever was additionally coated with 10 μm photoresist. Swelling of the photoresist layer in presence of water vapor provided sensor responses that were nearly proportional to R.H.% in the range of 2% to 60%. The reference cantilever provided temperature compensation and could also be used for temperature measurements.[117] The reference channel is also useful to minimize effects of other noise sources. It should be noted, however, that the photoresist coating used in these studies was not highly specific to water vapor and responded to alcohol vapor as well.[117] In the case of ethanol, concentration levels as low as 10 ppm could be easily detected. Somewhat different responsivities were obtained in the case of methanol, ethanol and 2-propanol.

In analogy to chemical sensors based on surface acoustic wave (SAW) transducers,[110] cantilevers coated with various commercially available polymers were proposed for distinguishing between different volatile organic compounds (VOCs) in air. Berger *et al.*[30] and Baller *et al.*[119] reported on a multicantilever sensor, in which signals were collected in a quasisimultaneous (time-multiplexing) manner from eight individual cantilever transducers, each modified with a different coating.[207,213–215] This design allowed the researchers to transfer the concept of a ''chemical nose'' from more conventional transduction principles[2] to innovative nanomechanical devices. Poly-methylmethacrylate (PMMA) as well as Pt metal coatings were used in some of these studies in order to demonstrate versatility of the cantilever arrays. Using a cantilever sensor with a PMMA coating, responses to a series of alcohols were obtained in both resonance and static deflection mode. Based on the differences in the shapes of response curves (either static deflection or resonance frequency change plotted as a function of time), the presence of different alcohols could be differentiated. In this case, the observed selectivity was primarily related to the fact that alcohols with different molecular weight and/or molecular structure have different diffusion rates in the PMMA coating. Therefore, the use of a multicantilever array with different polymeric coatings was the next logical step in developing a ''chemical nose'' based upon the cantilever platform. It was shown that cantilevers coated with several readily available ''generic'' polymers, such as polymethylmethacrylate, polystyrene, polyurethane, and their blends or copolymers, respond differently to various VOCs.[207,213] By applying principal component or artificial neuron network analysis to response patterns from arrays of such polymer-modified cantilevers, the concept of an ''electronic nose'' was implemented.

Selectivity of cantilever gas sensors can also be controlled by coating the transducer surface with stationary phases developed for chemical separation applications, such as gas-chromatography (GC). Such coatings were previously used to impart chemical selectivity to sensors based on electroacoustic SAW transduces.[94] More recently, this approach has been extended to cantilever sensors.[128] In one study, thin films of commercially available GC polysilane phases, SP2340 (polycyano-phase) and OV25 (polymethyl-phenyl-phase) were deposited on one side of the Si cantilevers using a combination of spin-coating and FIB milling.[128] The thicknesses of both the polysilane film and the cantilever material were varied by adjusting the conditions of spin-coating and FIB milling. The selectivity pattern of polysilane coated Si cantilevers was assessed by measuring bending responses to a series of VOCs with different polarities. For 300 nm thick silicon cantilevers, maximal responses were observed with approximately 100 nm of the polysilane modifying coatings. Selectivity was shown to be consistent with a common GC phase classification scheme.[128]

In order to create cantilever sensors with even more distinctive selectivity patterns with regard to different classes of VOCs, sol-gel coatings as well as covalently attached or evaporated films of synthetic receptors were found to be useful.[10,129,180] Thin films of sol-gels were formed on one side of 600 nm thick silicon cantilevers using aqueous solutions of organosilane precursors and spin coating procedures.[129] The cantilevers with sol-gel coatings exhibited strong bending in response to vapors of polar VOCs, in particular ethanol, while sensitivity to less polar compounds was relatively low. Additional chemical modification of the sol-gel coated cantilevers with a hydrophobic organosilane (hexamethyldisilazane) resulted in partial reversal of this trend and an eightfold increase in the response to *n*-pentane (the least polar compound among the screened analytes). Despite these promising results, obtaining uniform coatings on cantilevers using spin coating procedures was challenging. Alternative methods of physical and chemical modification of microcantilever transducers for gas sensors were investigated by the authors of this review in the recent studies.[180] An ultrathin layer of thiol-modified receptors of the cyclodextrin family was formed preferentially on one side of gold coated cantilevers using self-assembling procedures similar to those used previously with other types of transducers with noble metal surfaces. The coatings of this type can be expected to provide the sensor specificity based on molecular recognition mechanisms as well as size exclusion effects. For instance, sensor responsivities varied for trichloroethylene, tetrachloroethylene, and 2,7-dimethylnaphthalene.[180] Covalent attachment of the reactive receptor molecules onto nanostructured noble metal surfaces was found to be particularly suitable for creating highly efficient cantilever sensors. In the case of cantilevers with smooth gold surfaces, the magnitude of cantilever responses was only moderate. However, dramatic enhancements of responses were achieved when the same receptor layers were deposited on cantilevers with nanostructured (granular) gold films.[135] Using cantilever sensors with nanostructured surfaces, LODs as low as 0.17 ppb and 0.28 ppm were obtained for, respectively, 2,7-dimethylnaphtalene and tetrachloroethylene.

A microcantilever chemical detection platform based on an array of piezoelectric microcantilevers was demonstrated by applying this platform to detection of ethanol vapor.[199] The presence of ethanol vapor was found to be manifested in Novolac-coated cantilevers as a decrease in resonant frequency.[199] The measured response was found to be four times larger than the response measured for the same cantilever in the presence of water vapor. Those studies have also shown that ethanol vapor causes an increase in *Q*-factor for the Novolac-coated cantilever, which we attribute to a loos-

ening of the uncured gel-like coating that ordinarily has a higher damping coefficient; another possible explanation is a stiffening of the Novolac due to swelling, but this is less likely since gram-sized samples of uncured Novolac were tested in the laboratory and were shown to dissolve in ethanol.[199] A similar but lesser effect was also observed with the Novolac coated cantilevers in water.[199]

More recently, microcantilevers were used for the detection of explosives.[134,216] Pinnaduwage *et al.*[216] reported detection of 10 to 30 ppt levels of pentaerythritol tetranitrate (PETN) and hexahydro-1,3,5-triazine (RDX) using commercially available cantilevers coated with a gold layer that was functionalized with a self-assembled monolayer of 4-mercaptobenzoic acid. Pinnaduwage *et al.* reported[216] that those measurements corresponded to a limit of detection of a few femto-grams. Lavrik *et al.*[134] used trimaterial cantilevers modified with a tert-butylcalix[6] arene coating and reported large bending responses in presence of vapor phase TNT and its analogs, 2-mononitrotoluene (2-MNT) and 2,4-dinitrotoluene (2,4-DNT). Lavrik *et al.* estimated that the noise limited TNT detection threshold was 520 ppt.[134] A different approach to the detection of explosives in air using uncoated cantilever was reported by Pinnaduwage *et al.*[217] Those workers utilized the deflagration of TNT in a small localized explosion on an uncoated piezoresistive microcantilever. After removing the TNT source, the TNT molecules were slowly desorbed from the cantilever, and could be heated above the deflagration point by applying a voltage pulse to a piezoresistor integrated in the cantilever. The presence of TNT could be detected due to a small deflagration[217] that occurred when the cantilever temperature reached the TNT deflagration point.

In addition to sensors that utilize static or dynamic (resonance) cantilever responses due to adsorption (or absorption) of analyte molecules, bimaterial cantilevers can detect local temperature changes associated with a chemical reaction that involves analyte molecules and is catalyzed by a catalyst on the cantilever surface. One of the first implementations of this detection scheme was reported by Barnes *et al.*[63] By measuring deflections of a 1.5 μm thick Si cantilever with a 0.4 μm Al coating heat flux generated by a gas-phase catalytic reaction between O_2 and H_2 over a Pt surface was detected. For a standard AFM bimaterial cantilever and AFM optical cantilever readout, the limits of detection were estimated to be 1 pJ of thermal energy and 10^{-5} K of local temperature differences.[63] Even higher sensitivity of this method can be achieved using modified silicon or silicon nitride cantilevers with increased thermal isolation between their active regions (catalytic areas) and supporting bases (''heat sinks''). When heat escape through the surrounding environment becomes the principal path for the heat exchange, the sensitivity of cantilever based calorimetric sensors reaches its fundamental limit. While practical applications of cantilever based calorimetric detectors that involve catalytic reactions can be somewhat limited, much more versatile detection and identification of species adsorbed on cantilevers can be achieved using photothermal spectroscopy methods.[218–220] For instance, the authors of this review showed that analytes present on cantilevers in a form of thin coatings (about 100 nm average thickness) can be detected in a calorimetric spectroscopy mode.[219,220] While such cantilever based spectroscopic instruments may not satisfy rigorous definitions of chemical sensors they offer excellent portability combined with inherent to vibrational spectroscopy differentiating power.

We should point out that the static bending mode was used extensively in the majority of studies on cantilever sensors. However, resonating cantilevers scaled down to the nanoscale offer uniquely high mass sensitivity that cannot be achieved by using the static bending mode.[74] Therefore, resonating nanocantilevers may be indispensable in applications where species to be detected and analyzed are available in very minute quantities.

B. Liquid phase analytes

Early works on cantilever based chemical detection in liquids involved standard AFM cantilevers and AFM heads for their readout. Butt *et al.*[221] studied responses of 190 μm long, 0.6 μm thick, gold coated, silicon nitride AFM cantilevers to various chemical factors and found that the steady state deflections depend upon both pH and ionic strength of the aqueous medium. The ionic strength was varied by adjusting the concentration of KNO_3 varied from 0 to 1 M. The pH calibration plot acquired in 0.1 M KNO_3 was represented by two roughly linear regions corresponding to pH of 2–5.5 and pH of 8–11, respectively. This broad calibration plot with a relatively flat region at pH of 5.5–8 is qualitatively consistent with existing models of silicon nitride surface dissociation.[221] The average slope of the calibration curve was approximately 9 nm per pH (at 0.1 M KNO_3). Further research in this direction focused on surface modifications of cantilevers that can lead to improved or modified pH sensitivity. Alkylthiols terminated with different chemical groups were most extensively used as modifying agents for gold-coated cantilevers. The other modification procedures involved silane-oxide chemistry and spontaneous oxidation of evaporated aluminum films. When pH responses of cantilevers modified with carboxylic acid, hydroxyl, and amino groups were analyzed in several independent studies,[100,182] reasonable correlation between the experimental calibration plots and expected protonation-deprotonation behavior of the cantilever surfaces was found. The reported pH responsivities varied from 15 to 50 nm/pH and was dependent on the surface treatment, cantilever type, and pH range.

Some of the most impressive figures of merit demonstrated with cantilever sensors are related detection of heavy metal ions. In particular, Ji *et al.*[222] reported on highly sensitive and selective detection of Cs^+ ions using a cantilever sensor with a self-assembled responsive layer of the molecular recognition type. The responsive layer for this sensor was formed using a synthesized receptor compound which combined calixarene and crown-ether macrocycles and had a reactive-SH group that provided its covalent attachment to gold surfaces. Using a cantilever transducer with this responsive layer, Cs^+ ions could be detected in the concentration range of 10^{-11} to 10^{-7} M. The observed cantilever deflections in response to Cs^+ ions reached a steady state in less

than 5 min. Cantilever deflections up to 350 nm were documented in this study. Importantly, Na^+ ions had almost no effect on the cantilever bending while rather good selectivity was observed with respect to K^+ (a steady state response of 115 nm corresponded to 5×10^{-10} M Cs^+ or 10^{-4} M K^+). By modifying gold coated cantilever transducers with another self-assembled responsive monolayer, triethyl-12-mercaptododecylammonium bromide, a detector of trace amounts of CrO_4^{2-} was implemented.[181] It was reported that, while 10^{-9} M CrO_4^{2-} could be detected, other anions, such as Cl^-, Br^-, CO_3^{2-}, and SO_4^{2-}, had a minimal affect on the sensor response. As an extension of this approach, detection of trace levels of Ca^{2+} was also achieved using cantilever transducers modified with Ca^{2+} selective self-assembled responsive layers.[141] Two alternative chemical functionalization procedures were used in this study and resulted in the two kinds of self-assembled monolayers terminated with, respectively, with phosphate and N,N-diethyl-acetamide moieties. Cantilever sensors with these two types of selective coatings were shown to be practically useful in complementary ranges of Ca^{2+} concentrations spanning from 10^{-9} to 10^{-2} M. At the same time, Na^+ and K^+ cations at their physiological concentrations had negligible interfering effect on these sensors. Self-assembled monolayers of yet another long-chain thiol compound were found to improve selectivity of gold coated cantilevers towards Hg^{2+} cations. Hg^{2+} at concentrations as low as 10^{-11} could be detected using this approach, while other cations, such as K^+, Na^+, Pb^{2+}, Zn^{2+}, Ni^{2+}, Cd^{2+}, Cu^{2+}, and Ca^{2+} had little or no effect on the cantilever deflections.

Cantilevers modified with synthetic receptor compounds of the molecular recognition type were also found to be useful for detection of various neutral aromatic compounds in aqueous solutions.[136,223] In particular, self-assembled monolayers of a thiolated beta-cyclodextrin derivative and evaporated thin films of heptakis (2,3-O-diacetyl-6-O-tertbutyldimethylsilyl)-beta-cyclodextrin were studied on smooth and nanostructured gold-coated microcantilever surfaces. In those studies, micro- and nano-structural modifications of microcantilevers chemical sensors were shown to improve the stress transduction between the chemical coating and the transducer. Structural modifications of microcantilever surfaces were achieved using either chemical dealloying[136] or focused ion beam milling.[223] The dealloyed surfaces[133,135,136,180,223] contained nanometer-sized features that enhanced the transduction of molecular recognition events into cantilever response, as well as increased coatings stability in the case of thicker films. The observed response factors for the analytes studied varied from 0.02–604 nm/ppm. Calibration plots obtained for 2,3-dihydroxynaphthalene and several volatile organic compounds revealed proportionality between the analyte concentrations and cantilever deflections in the range of up to several hundred nanometers. By manipulating surface morphologies and film thicknesses, improvements in the limits of detection as great as 2 orders of magnitude were demonstrated.[136,223]

C. Biosensors

An attempt to combine the biosensor concept and a cantilever transducer took advantage of the ultrahigh calorimetric sensitivity of a bimaterial microcantilever.[10,218] By immobilizing glucose oxidize on the surface of 320-μm long, gold coated silicon nitride cantilevers, Subramanian *et al.* created a glucose sensor that responded to presence of glucose in the aqueous medium due to the enzyme-induced exothermic processes.[224] This sensor exhibited a good linear calibration curve for glucose concentrations in the range of 5–40 mM. Specificity of the sensor to glucose was confirmed in control experiments, in which responses to mannose were approximately 25% of responses to glucose of the same concentration. Control experiments also revealed subtle glucose responsivity of the cantilever transducer without immobilized enzyme.

Another indirect method of detecting biological species using micromachined cantilevers was proposed by Baselt and coworkers.[225,226] Their force amplified biological sensor (FABS) utilized a micromachined cantilever placed in a strong magnetic field. Similar to many conventional biological assays, such as the enzyme-linked immunosorbent assay, the FABS method relied on labeled biological material, however, magnetic beads rather than enzymes or fluorophores were used as a label. It was shown that an important advantage of the FABS method over existing bioassays is its capability to detect trace amounts of extremely dilute biological samples.

More recently, significant attention has been drawn to direct conversion of various biological receptor-ligand interactions into mechanical responses using cantilever transducers.[31,33,101,179,227–233] Raiteri *et al.* explored high sensitivity of cantilever transducers to interfacial stress changes[227] in their work on a biosensor for a herbicide. The researchers reported bending responses of microfabricated cantilevers associated with interaction between the surface-immobilized herbicide (2,4-dichlorophenoxyacetic) and the monoclonal antiherbicide antibody in an aqueous solution. The optical lever method was used to monitor deflections of a cantilever placed in a liquid flow-through cell with a flow rate of 0.5 mL/min that was provided by a peristaltic pump. In the described experiments, standard gold coated silicon nitride AFM cantilevers were successively incubated in cysteamine and glutaraldehyde solutions in order to activate them for preferential binding of the 2,4-dichlorophenoxyacetic-albumin conjugate on the gold surface. The cantilever with thus immobilized herbicide exhibited partially reversible bending in response to the antiherbicide antibodies at the concentrations of 5 and 25 μg/mL in a phosphate buffer saline. The magnitude of the measured responses was about 50 nm, which significantly exceeded the readout accuracy (0.1 nm). Unfortunately, no clear correlation between the antibody concentration and the bending magnitude was observed in this study.

Despite the excellent sensitivity of cantilever transducers and their capability to detect receptor-ligand interactions directly, the static deflection mode is not free from long-term drifts and instabilities inherent to other types of biosensors.

In addition to temperature-induced drifts, it was also established that both specific binding and nonspecific adsorption of proteins on various surfaces are accompanied with very slow surface stress changes.[230] Moulin *et al.*[230] used microfabricated cantilevers to measure surface stress changes associated with nonspecific adsorption of immunoglobulin G (IgG) and bovine serum albumin (BSA) on gold surfaces. Compressive and tensile surface stress changes were observed upon adsorption of, respectively, IgG and BSA. This difference was attributed to different packing and deformation of each protein on the gold surface. It was also concluded that biological assays based on surface stress measurements are sensitive to subtle differences in preparation and purification of proteins that are otherwise identical and cannot be differentiated using other techniques.[230] Taking into account extremely high sensitivity of cantilever bending to interfacial biomolecular binding events, Moulin *et al.*[31] proposed a clinically relevant cantilever biosensor for differentiation of low density lipoproteins (LDL) and their oxidized form (oxLDL). For this purpose, silicon nitride cantilevers with freshly evaporated gold were modified with heparin. The modification procedure included successive incubation of the cantilevers in 2-aminoethanethiol hydrochloride and heparin solutions, and saturation of nonspecific binding sites with BSA (each incubation was followed by rinsing in purified water). The resulting cantilevers exhibited pronounced bending in opposite directions upon exposure to 120 μg/mL of LDL and 10 μg/mL of oxLDL, respectively. The adsorption induced surface stress changes measured using the cantilever biosensor were notably slower in comparison to the binding kinetics observed in the control surface plasmon resonance measurements. Therefore, a conclusion can be made that post-adsorption molecular rearrangement processes play an important role in generating prolonged responses of the cantilever sensor.

A significant milestone in developing cantilever based biosensors was demonstration of their applicability to DNA analysis.[101,179,232,233] Fritz *et al.* reported on sensitive and specific monitoring of oligonucleotide hybridization using arrays of functionalized cantilevers and optical readout of their deflections.[101] Arrays of 1 μm thick, 500 μm long rectangular silicon cantilevers, custom designed and microfabricated at IBM Zurich Research Laboratory (Ruschlikon, Switzerland) were used in these studies. A thin layer of gold on one side of the cantilevers permitted controllable immobilization of thiomodified oligonucleotides. When 12-mer oligonucleotides with different degree of complementarity were used in the hybridization assay, a single base pair mismatch was clearly detectable. The use of a differential pair of cantilever transducers, i.e., functionalized and ''blank,'' and analysis of the differential deflections was an important refinement that minimized interfering effects of temperature, mechanical vibrations, and fluid flow in the cell and, therefore, provided more reliable differentiation of the responses that accompanied specific biomolecular interactions. The residual noise in the differential signal corresponded to approximately 0.5 nm. The LOD of the proposed method defined on the basis of this noise was estimated to be 10 nM. In addition to oligonucleotide hybridization assays, differential cantilever deflection method was shown to be very promising for monitoring a wide range of biological affinity interactions. In particular, irreversible differential responses were observed in the course of protein A–IgG interactions.[31] In a similar study reported by Raiteri *et al.*,[228] 85 ng/mL myoglobin in an aqueous solution was detected using a differential pair of cantilevers, one of which was functionalized with monoclonal antimyoglobin antibodies.

Nevertheless, under carefully controlled experimental conditions (temperature, pH, ionic strength, etc.), even a single cantilever transducer provides a sensitive means for detection of various biomolecular interactions. For instance, Thundat and coworkers succeeded in differentiating a single-nucleotide mismatch using a cantilever transducer placed in a thermally stabilized flow cell.[179,232] Within approximately 30 to 60 min after the sample injection, the cantilever deflections reached a steady state that was typically in the range of -25 to 10 nm. Both the rate and the magnitude of deflection response were dependent on the length and sequence mismatch of the analyzed oligonucleotide. The same group of researchers also reported[232] on detection of ultralow concentrations (0.2 ng/ml) of prostate specific antigen (PSA) using a similar thermoelectrically stabilized cell housing a single cantilever transducer. In that clinically relevant study, the calibration curve for PSA at the concentrations of 10^{-2} to 10^{6} ng/mL was measured using a series of similar cantilever transducers and plotted in terms of the generated surface stress change. It is important to emphasize that background buffered solutions in these experiments contained physiological levels (1 mg/mL) of both human serum albumin and human plasminogen, thus making the reported results especially clinically relevant.

Biotin-streptavidin is yet another example of high-affinity biomolecular interactions that was successfully monitored using cantilever transducers. Raiteri *et al.* used biotin functionalized silicon nitride cantilevers and measured their deflection responses in presence of 100 nM streptavidin.[228] These responses that reached approximately 50 nm in magnitude within 10 min were largely reversible. In the case of high-affinity streptavidin-biotin interactions, the reversible nature of the responses is especially unexpected and apparently indicates a nontrivial relationship between the surface coverage of streptavidin molecules on the cantilever surface and the associated surface stress change.

It is important to note that the deflection responses of cantilever based biosensors rarely exceed 100 nm regardless of the chosen biological affinity system. This implies that signal-to-noise ratios and sensitivities achievable with conventionally designed cantilever biosensors may be limited by common fundamental mechanisms. A question arises as to whether such limitations can be surmounted. Recent studies conduced by the authors of this article addressed this question by exploring cantilevers with asymmetrically nanostructured surfaces and demonstrated feasibility of cantilever biosensors with dramatically enhanced responsivities. It was found that interfacial biomolecular recognition events were converted into mechanical responses much more efficiently when high density of nanosize features were present on one side of the cantilever transducers. Creating of such interfaces

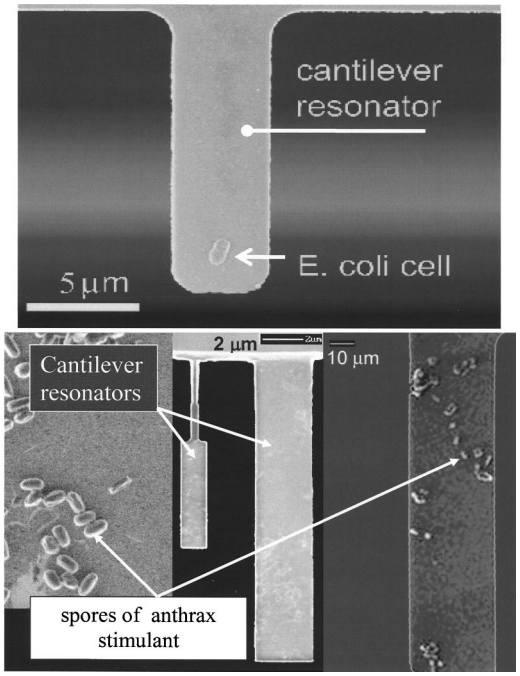

FIG. 13. Resonating cantilever devices that provide mass sensitivity sufficient for a single cell detection. These sensors were described in studies by (a) Ilic *et al.* (Ref. 105) and (b) Lavrik and Datskos (Ref. 74).

may rely on surface immobilization of gold nanospheres or dealloying of coevaporated Au:Ag films. The most efficient transduction was achieved when the cantilevers were modified with 50 to 75 nm thick dealloyed Au:Ag films. Unlike conventional cantilevers with smooth surfaces, these nanostructured transducers exhibited up to several micron deflections upon adsorption of protein A and biotin-labeled albumin on nanostructured gold surfaces. Additional micrometer scale deflections of the cantilevers were observed upon interaction of the surface immobilized receptors with, respectively, immunoglobulin G and avidin.[10]

Yet, another promising approach to ultrasensitive detection of biological species in air was demonstrated by Ilic *et al.* using smaller cantilevers operating in the resonance mode.[105,234] The silicon nitride cantilevers used in these studies were about 5 μm long, had resonance frequencies in the megahertz range, and permitted detection of minute amounts of biological molecules or cells. In Fig. 13 (top image), we show a micrograph of the cantilever used by Ilic *et al.* where a single E. coli cell is present at the tip of the cantilever. Mass sensitivity of the designed cantilever sensor was sufficient to detect mass changes due to attachment of a single microbial cell while modification of the cantilever surface with appropriate biological receptors, for instance antibodies, provided high detection specificity.

VII. DISCUSSION

Cantilever transducers are recognized as a promising platform for the next generation of chemical and biological sensors. It is anticipated that microfabricated cantilevers can provide a versatile platform for real-time, *in situ* measurements of physical, chemical, and biochemical properties of physiological fluids. In general, the MEMS platform offers an unparalleled capability for the development and mass production of extremely sensitive, low-cost sensors suitable for rapid analysis of many chemical and biological species. Compared with more conventional sensors, cantilever sensors offer improved dynamic response, greatly reduced size, high precision, and increased reliability. A plethora of physical, chemical, and biological sensors based on the micromachined cantilever transducers have already been demonstrated.[7,30,45,63,66,115,119,136,137,207,218,137,207,218]

An important advantage of microcantilever sensors is that they can operate in vacuum, gases, and liquids. A compelling feature of the cantilever-based sensors operating in the resonant mode is that four response parameters (resonance frequency, phase, amplitude, and *Q*-factor, measured simultaneously) may provide complementary information about the interactions between the sensor and the environment. The damping effects of a liquid medium, however, reduce resonance responses of cantilever devices. In most common liquids, such as aqueous solutions, the amplitude of the cantilever oscillations at the resonance can be orders of magnitude lower as compared to the same resonating cantilever operating in air. On the other hand, operation in the static mode is unaffected by viscous properties of the medium. Therefore, microcantilever sensors operating in the static mode are especially attractive as a platform for nanomechanical biochemical assays and other biomedical applications.

Another unique advantage of cantilever sensors is that deformations and resonance frequency shifts measured simultaneously provide complementary information about the interactions between the transducers and the environment. Micro- and nano-scale cantilevers have extremely small thermal masses and can be heated and cooled with thermal time constants of less than a millisecond. This is advantageous for rapid reversal of molecular absorption processes and regeneration purposes. Both static and dynamic responses of cantilever sensors can be measured with very high precision using several readout techniques[46] based on optical beam deflection, interferometry, electron transfer, piezoresistance, capacitance, and piezoelectric properties. Other resonance parameters of cantilever transducers, such as amplitude and *Q*-factor, can be extracted from these responses measured in an appropriate frequency or time domain.

Cantilevers operating in the static mode often surpass in performance cantilevers operating in the resonant operation. However, the mass sensitivity of cantilever transducers operating in the resonance mode increases as their dimensions are reduced. Therefore, cantilever sensors with progressively increased mass sensitivity can be fabricated by simply reducing the transducer dimensions.[74,151,235,236] As the technology of nanosize mechanical structures advances, nanomechanical devices approach the gigahertz frequency domain that is already widely explored with electronic and optical devices. In order to achieve fundamentally limited performance of resonating cantilever sensors, it is necessary to delineate the noise present in micromechanical systems. The type of noise in cantilever devices referred to as ''thermomechanical''[46,148] or ''mechanical-thermal noise''[237,238] arises from the dynamic equilibrium between mechanical energy of the device

and thermal energy of the surrounding environment at nonzero temperatures. This type of noise imposes the ultimate limits on the performance of microcantilever sensors operating in the resonance mode.

The advantages of cantilever sensors can be further expanded by arranging individual cantilever transducers into large multisensor arrays integrated with on-chip electronic circuitry.[239] One-dimensional and two-dimensional arrays of cantilever transducers offer additional advantages that cannot be overlooked. In particular, such arrays provide a viable platform for the development of high-performance ''electronic noses.''

ACKNOWLEDGMENTS

The authors would like to acknowledge support from the Defense Advanced Research Projects Agency, the National Science Foundation, and the U.S. Department of Energy. This work was performed in part at the Cornell Nanofabrication Facility (a member of the National Nanofabrication Users Network) which is supported by the National Science Foundation under Grant No. ECS-9731293, Cornell University and industrial affiliates. This work was partially supported by the Laboratory Director's Research and Development Program of Oak Ridge National Laboratory. Oak Ridge National Laboratory is operated for the U.S. Department of Energy by UT-Battelle under contract DE-AC05-96OR22464.

[1] J. Janata, *Principles of Chemical Sensors* (Plenum, New York, 1989).
[2] J. Janata, M. Josowicz, and D. M. Devaney, Anal. Chem. **66**, R207 (1994).
[3] J. Janata, Anal. Chem. **62**, 33R (1990).
[4] G. T. A. Kovacs, *Micromachined Transducers* (McGraw-Hill, New York, 1998).
[5] R. Berger, H. P. Lang, C. Gerber, J. K. Gimzewski, J. H. Fabian, L. Scandella, E. Meyer, and H.-J. Guntherodt, Chem. Phys. Lett. **294**, 363 (1998).
[6] E. A. Wachter and T. Thundat, Rev. Sci. Instrum. **66**, 3662 (1995).
[7] V. Ferrari, D. Marioli, A. Taroni, E. Ranucci, and P. Ferruti, IEEE Trans. Ultrason. Ferroelectr. Freq. Control **43**, 601 (1996).
[8] A. M. Moulin, R. J. Stephenson, and M. E. Welland, J. Vac. Sci. Technol. B **15**, 590 (1997).
[9] H. L. Tuller and R. Mlcak, Curr. Opin. Solid State Mater. Sci. **3**, 501 (1998).
[10] P. G. Datskos, M. J. Sepaniak, C. A. Tipple, and N. Lavrik, Sens. Actuators B **76**, 393 (2001).
[11] M. Sepaniak, P. Datskos, N. Lavrik, and C. Tipple, Anal. Chem. **74**, 568A (2002).
[12] G. Binnig, C. F. Quate, and C. Gerber, Phys. Rev. Lett. **56**, 930 (1986).
[13] S. P. Timoshenko, J. Opt. Soc. Am. **11**, 233 (1925).
[14] F. J. Norton, U.S. Patent No. 2,307,800 (1943).
[15] P. J. Shaver, Rev. Sci. Instrum. **40**, 901 (1969).
[16] W. E. Newell, Science **161**, 1320 (1968).
[17] I. Steinberg, A. Oplatka, and A. Katchalsky, Nature (London) **210**, 568 (1966).
[18] A. Katchalsky, I. Steinberg, A. Oplatka, and A. Kam, U.S. Patent No. 3321908 (1967).
[19] W. G. Palmer, Proc. R. Soc. London, Ser. A **106**, 55 (1924).
[20] J. E. Sears, Sci. Mon. **20**, 427 (1925).
[21] F. T. Meehan, Proc. R. Soc. London, Ser. A **115**, 199 (1927).
[22] D. H. Bangham and N. Fakhoury, Proc. R. Soc. London, Ser. A **130**, 81 (1930).
[23] R. V. Jones and C. W. McCombie, Philos. Trans. R. Soc. London, Ser. A **244**, 205 (1952).
[24] H. C. Nathanson, W. E. Newell, and R. A. Wickstrom, Electronics **38**, 84 (1965).
[25] M. Nonnenmacher, J. Greschner, O. Wolter, and R. Kassing, J. Vac. Sci. Technol. B **9**, 1358 (1991).
[26] D. A. Walters, J. P. Cleveland, N. H. Thomson, P. K. Hansma, M. A. Wendman, G. Gurley, and V. Elings, Rev. Sci. Instrum. **67**, 3583 (1996).
[27] A. N. Cleland and M. L. Roukes, Appl. Phys. Lett. **69**, 2653 (1996).
[28] R. Giles, J. P. Cleveland, S. Manne, P. K. Hansma, B. Drake, P. Maivald, C. Boles, J. Gurley, and V. Elings, Appl. Phys. Lett. **63**, 617 (1993).
[29] T. Thundat, P. I. Oden, and R. J. Warmack, Microscale Thermophys. Eng. **1**, 185 (1997).
[30] R. Berger, C. Gerber, H. P. Lang, and J. K. Gimzewski, Microelectron. Eng. **35**, 373 (1997).
[31] A. M. Moulin, S. J. O'Shea, and M. E. Welland, Ultramicroscopy **82**, 23 (2000).
[32] H. G. Craighead, Science **290**, 1532 (2000).
[33] R. D. Pereira, Biochem. Pharmacol. **62**, 975 (2001).
[34] H. Fujita and H. Toshiyoshi, IEICE Trans. Electron. **E83C**, 1427 (2000).
[35] J. M. Zara and S. W. Smith, Sens. Actuators, A **102**, 176 (2002).
[36] M. Kim, J. B. Hacker, R. E. Mihailovich, and J. E. DeNatale, IEEE Microw. Wirel. Compon. Lett. **11**, 56 (2001).
[37] J. A. Walker, J. Micromech. Microeng. **10**, R1 (2000).
[38] R. Wood, R. Mahadevan, V. Dhuler, B. Dudley, A. Cowen, E. Hill, and K. Markus, Mechatronics **8**, 535 (1998).
[39] P. Vettiger, J. Brugger, M. Despont, U. Drechsler, U. Durig, W. Haberle, M. Lutwyche, H. Rothuizen, R. Stutz, R. Widmer, and G. Binnig, Microelectron. Eng. **46**, 11 (1999).
[40] P. Vettiger, M. Despont, U. Drechsler, U. Durig, W. Haberle, M. I. Lutwyche, H. E. Rothuizen, R. Stutz, R. Widmer, and G. K. Binnig, IBM J. Res. Dev. **44**, 323 (2000).
[41] H. Kawakatsu, D. Saya, A. Kato, K. Fukushima, H. Toshiyoshi, and H. Fujita, Rev. Sci. Instrum. **73**, 1188 (2002).
[42] M. I. Lutwyche, M. Despont, U. Drechsler, U. Durig, W. Haberle, H. Rothuizen, R. Stutz, R. Widmer, G. K. Binnig, and P. Vettiger, Appl. Phys. Lett. **77**, 3299 (2000).
[43] L. R. Carley, J. A. Bain, G. K. Fedder, D. W. Greve, D. F. Guillou, M. S. C. Lu, T. Mukherjee, S. Santhanam, L. Abelmann, and S. Min, J. Appl. Phys. **87**, 6680 (2000).
[44] H. Shin, S. Hong, J. Moon, and J. U. Jeon, Ultramicroscopy **91**, 103 (2002).
[45] T. Thundat, P. I. Oden, P. G. Datskos, G. Y. Chen, and R. J. Warmack, in *The 16th Warner Brandt Workshop on Charged Particle Penetration Phenomena*, Oak Ridge Tennessee, 1996 (Oak Ridge National Laboratory, Oak Ridge, TN, 1996).
[46] D. Sarid, *Scanning Force Microscopy* (Oxford University Press, New York, 1991).
[47] H. J. Butt, J. Colloid Interface Sci. **180**, 251 (1996).
[48] J. Samuel, C. J. Brinker, L. J. D. Frink, and F. van Swol, Langmuir **14**, 2602 (1998).
[49] L. J. D. Frink and F. van Swol, Colloids Surf., A **162**, 25 (2000).
[50] J. E. Sader, J. Appl. Phys. **91**, 9354 (2002).
[51] J. E. Sader, J. Appl. Phys. **89**, 2911 (2001).
[52] M. Godin, V. Tabard-Cossa, P. Grutter, and P. Williams, Appl. Phys. Lett. **79**, 551 (2001).
[53] R. Raiteri, H. J. Butt, and M. Grattarola, Electrochim. Acta **46**, 157 (2000).
[54] K. J. Bruland, J. L. Garbini, W. M. Dougherty, and J. A. Sidles, J. Appl. Phys. **83**, 3972 (1998).
[55] D. Rugar, C. S. Yannoni, and J. A. Sidles, Nature (London) **360**, 563 (1992).
[56] H. J. Mamin and D. Rugar, Appl. Phys. Lett. **79**, 3358 (2001).
[57] P. Streckeisen, S. Rast, C. Wattinger, E. Meyer, P. Vettiger, C. Gerber, and H. J. Guntherodt, Appl. Phys. A: Mater. Sci. Process. **66**, S341 (1998).
[58] A. N. Cleland and M. L. Roukes, Nature (London) **392**, 160 (1998).
[59] A. C. Stephan, T. Gaulden, A. D. Brown, M. Smith, L. F. Miller, and T. Thundat, Rev. Sci. Instrum. **73**, 36 (2002).
[60] A. Erbe, R. H. Blick, A. Tilke, A. Kriele, and J. P. Kotthaus, Appl. Phys. Lett. **73**, 3751 (1998).
[61] D. V. Scheible, A. Erbe, and R. H. Blick, New J. Phys. **4**, 86.1 (2002).
[62] P. G. Datskos and T. Thundat, J. Nanosci. Nanotechnol. **2**, 369 (2002).
[63] J. R. Barnes, R. J. Stephenson, M. E. Welland, C. Gerber, and J. K. Gimzewski, Nature (London) **372**, 79 (1994).
[64] R. Berger, C. Gerber, J. K. Gimzewski, E. Meyer, and H. J. Guntherodt, Appl. Phys. Lett. **69**, 40 (1996).
[65] P. I. Oden, P. G. Datskos, T. Thundat, and R. J. Warmack, Appl. Phys. Lett. **69**, 3277 (1996).

[66] E. A. Wachter, T. Thundat, P. I. Oden, R. J. Warmack, P. G. Datskos, and S. L. Sharp, Rev. Sci. Instrum. **67**, 3434 (1996).
[67] P. G. Datskos, S. Rajic, and I. Datskou, Appl. Phys. Lett. **73**, 2319 (1998).
[68] R. Amantea, L. A. Goodman, F. Pantuso, D. J. Sauer, M. Varhese, T. S. Villianni, and L. K. White, Infrared Technology and Applications XXIV **3436**, 647 (1998).
[69] T. Perazzo, M. Mao, O. Kwon, A. Majumdar, J. B. Varesi, and P. Norton, Appl. Phys. Lett. **74**, 3567 (1999).
[70] M. Mao, T. Perazzo, O. Kwon, Y. Zhao, A. Majumdar, J. Varesi, and P. Norton, in *Microelectromechanical Systems*, edited by Y. C. Lee, K. Goodson, R. S. Keynton, A. Lee, L. Lin, and F. K. Forster (The American Society of Mechanical Engineers, Nashville, TN, 1999), Vol. 1, p. 309.
[71] P. G. Datskos, S. Rajic, and I. Datskou, Ultramicroscopy **82**, 49 (2000).
[72] L. R. Senesac, J. L. Corbeil, N. V. Lavrik, S. Rajic, and P. G. Datskos, Ultramicroscopy **97**, 451 (2003).
[73] R. G. Knobel and A. N. Cleland, Nature (London) **424**, 291 (2003).
[74] N. V. Lavrik and P. G. Datskos, Appl. Phys. Lett. **82**, 2697 (2003).
[75] D. J. C. Yates, Proc. R. Soc. London, Ser. A **224**, 526 (1954).
[76] W. Kuhn, Nature (London) **165**, 514 (1950).
[77] M. V. Sussman and A. Katchalsky, Science **167**, 45 (1970).
[78] D. Dye, Proc. R. Soc. London, Ser. A **103**, 240 (1923).
[79] E. H. Taylor and W. C. Waggener, J. Phys. Chem. **83**, 1361 (1979).
[80] D. R. Baselt, B. Fruhberger, E. Klaassen, S. Cemalovic, C. L. Britton, S. V. Patel, T. E. Mlsna, D. McCorkle, and B. Warmack, Sens. Actuators B **88**, 120 (2003).
[81] R. Shuttleworth, Proc. Phys. Soc. London **63A**, 444 (1950).
[82] R. V. Jones, Proc. R. Soc. London, Ser. A **249**, 100 (1959).
[83] W. E. Newell, Proc. IEEE **52**, 1603 (1964).
[84] W. E. Newell, R. A. Wickstrom, and D. J. Page, *Proceedings of the IEEE International Meeting on Electron Devices* (Washington, DC, 1967), p. 24.
[85] W. E. Newell, R. A. Wickstrom, and D. J. Page, IEEE Trans. Electron Devices **ED15**, 411 (1968).
[86] W. E. Newell, Proc. IEEE **53**, 575 (1965).
[87] I. Koga, J. Appl. Phys. **34**, 2357 (1963).
[88] E. P. Scheide and J. K. Taylor, Environ. Sci. Technol. **8**, 1097 (1974).
[89] E. P. Scheide and J. K. Taylor, Am. Ind. Hyg. Assoc. J. **36**, 897 (1975).
[90] E. P. Scheide and R. J. Warnar, Am. Ind. Hyg. Assoc. J. **39**, 745 (1978).
[91] J. W. Grate, A. Snow, D. S. Ballantine, Jr., H. Wohltjen, M. H. Abraham, R. A. McGill, and P. Sasson, Anal. Chem. **60**, 869 (1988).
[92] J. W. Grate, S. J. Martin, and R. M. White, Anal. Chem. **65**, 940A (1993).
[93] M. Rap, P. Binz, I. Kabbe, M. Van Schickfus, H. Hunklinger, A. Fuchs, W. Schepp, and B. Fleischmann, Sens. Actuators B **4**, 103 (1991).
[94] J. W. Grate and M. Klusky, Anal. Chem. **63**, 1719 (1991).
[95] M. D. Ward and D. A. Buttry, Science **249**, 1000 (1990).
[96] J. Burov and V. Hinkov, Opt. Quantum Electron. **7**, 474 (1975).
[97] M. I. Borisov, V. P. Hinkov, J. I. Burov, V. Strashilov, and K. P. Bransalov, Int. J. Electron. **39**, 377 (1975).
[98] H. C. Nathanson, W. E. Newell, R. A. Wickstrom, and J. R. Davis, IEEE Trans. Electron Devices **ED14**, 117 (1967).
[99] W. E. Newell and R. A. Wickstrom, IEEE Trans. Electron Devices **ED16**, 781 (1969).
[100] J. Fritz, M. K. Baller, H. P. Lang, T. Strunz, E. Meyer, H. J. Guntherodt, E. Delamarche, C. Gerber, and J. K. Gimzewski, Langmuir **16**, 9694 (2001).
[101] J. Fritz, M. K. Baller, H. P. Lang, H. Rothuizen, P. Vettiger, E. Meyer, H. J. Guntherodt, C. Gerber, and J. K. Gimzewski, Science **288**, 316 (2000).
[102] P. G. Datskos, C. M. Egert, and I. Sauers, Sens. Actuators B **61**, 75 (2000).
[103] R. Berger, E. Delamarche, H. P. Lang, C. Gerber, J. K. Gimzewski, E. Meyer, and H. J. Guntherodt, Appl. Phys. A: Mater. Sci. Process. **66**, S55 (1998).
[104] P. I. Oden, Sens. Actuators B **53**, 191 (1998).
[105] B. Ilic, D. Czaplewski, M. Zalalutdinov, H. G. Craighead, P. Neuzil, C. Campagnolo, and C. Batt, J. Vac. Sci. Technol. B **19**, 2825 (2001).
[106] H. C. Nathanson and R. A. Wickstrom, Appl. Phys. Lett. **7**, 84 (1965).
[107] J. W. Grate, S. W. Wenzel, and R. M. White, Anal. Chem. **63**, 1552 (1991).
[108] J. W. Grate, S. J. Martin, and R. M. White, Anal. Chem. **65**, A987 (1993).
[109] J. W. Grate and R. A. McGill, Anal. Chem. **67**, 4015 (1995).
[110] J. W. Grate, *Surface-Acoustic Wave Array Detectors* (Report No. DOE/EM-0254, 1995).
[111] R. E. Martinez, W. M. Augustyniak, and J. A. Golovchenko, Phys. Rev. Lett. **64**, 1035 (1990).
[112] H. Ibach, J. Vac. Sci. Technol. A **12**, 2240 (1994).
[113] G. G. Stoney, Proc. R. Soc. London, Ser. A **82**, 172 (1909).
[114] S. Timoshenko, *Theory of Plates and Shells* (McGraw-Hill, New York, 1940).
[115] T. Thundat, E. A. Wachter, S. L. Sharp, and R. J. Warmack, Appl. Phys. Lett. **66**, 1695 (1995).
[116] J. Brugger, G. Beljakovic, M. Despont, N. F. deRooij, and P. Vettiger, Microelectron. Eng. **35**, 401 (1997).
[117] A. Boisen, J. Thaysen, H. Jensenius, and O. Hansen, Ultramicroscopy **82**, 11 (2000).
[118] C. L. Britton, R. L. Jones, P. I. Oden, Z. Hu, R. J. Warmack, S. F. Smith, W. L. Bryan, and J. M. Rochelle, Ultramicroscopy **82**, 17 (2000).
[119] M. K. Baller, H. P. Lang, J. Fritz, C. Gerber, J. K. Gimzewski, U. Drechsler, H. Rothuizen, M. Despont, P. Vettiger, F. M. Battiston, J. P. Ramseyer, P. Fornaro, E. Meyer, and H. J. Guntherodt, Ultramicroscopy **82**, 1 (2000).
[120] K. Dahmen, S. Lehwald, and H. Ibach, Surf. Sci. **446**, 161 (2000).
[121] F. J. von Preissig, J. Appl. Phys. **66**, 4262 (1989).
[122] T. Miyatani and M. Fujihira, J. Appl. Phys. **81**, 7099 (1997).
[123] W. L. Fang, J. Micromech. Microeng. **9**, 230 (1999).
[124] Z. Y. Hu, T. Thundat, and R. J. Warmack, J. Appl. Phys. **90**, 427 (2001).
[125] R. Koch, J. Phys.: Condens. Matter **6**, 9519 (1994).
[126] R. Koch, Appl. Phys. A: Mater. Sci. Process. **69**, 529 (1999).
[127] J. Israelachvili, *Intermolecular and Surface Forces* (Academic Press, San Diego, 1991).
[128] T. A. Betts, C. A. Tipple, M. J. Sepaniak, and P. G. Datskos, Anal. Chim. Acta **422**, 89 (2000).
[129] B. C. Fagan, C. A. Tipple, Z. L. Xue, M. J. Sepaniak, and P. G. Datskos, Talanta **53**, 599 (2000).
[130] B. Raguse, K. H. Muller, and L. Wieczorek, Adv. Mater. (Weinheim, Ger.) **15**, 922 (2003).
[131] D. Kaneko, J. P. Gong, and Y. Osada, J. Mater. Chem. **12**, 2169 (2002).
[132] R. H. Baughman, C. X. Cui, A. A. Zakhidov, Z. Iqbal, J. N. Barisci, G. M. Spinks, G. G. Wallace, A. Mazzoldi, D. De Rossi, A. G. Rinzler, O. Jaschinski, S. Roth, and M. Kertesz, Science **284**, 1340 (1999).
[133] N. V. Lavrik, C. A. Tipple, M. J. Sepaniak, and P. G. Datskos, Chem. Phys. Lett. **336**, 371 (2001).
[134] L. V. Lavrik, M. J. Sepaniak, and P. G. Datskos, Sens. Lett. **1**, 25 (2003).
[135] N. V. Lavrik, C. A. Tipple, M. J. Sepaniak, and P. G. Datskos, Biomed. Microdevices **3**, 33 (2001).
[136] C. A. Tipple, N. V. Lavrik, M. Culha, J. Headrick, P. Datskos, and M. J. Sepaniak, Anal. Chem. **74**, 3118 (2002).
[137] Z. J. Davis, G. Abadal, O. Kuhn, O. Hansen, F. Grey, and A. Boisen, J. Vac. Sci. Technol. B **18**, 612 (2000).
[138] P. G. Datskos and I. Sauers, Sens. Actuators B **61**, 75 (1999).
[139] Y. Martin, C. C. Williams, and H. K. Wickramasinghe, J. Appl. Phys. **61**, 4723 (1987).
[140] T. Thundat, R. J. Warmack, Chen, and D. P. Allison, Appl. Phys. Lett. **64**, 2894 (1994).
[141] S. Cherian, A. Mehta, and T. Thundat, Langmuir **18**, 6935 (2002).
[142] G. Y. Chen, T. Thundat, E. A. Wachter, and R. J. Warmack, J. Appl. Phys. **77**, 3618 (1995).
[143] G. Y. Chen, R. J. Warmack, T. Thundat, D. P. Allison, and A. Huang, Rev. Sci. Instrum. **65**, 2532 (1994).
[144] T. Thundat, G. Y. Chen, R. J. Warmack, D. P. Allison, and E. A. Wachter, Anal. Chem. **67**, 519 (1995).
[145] F. R. Blom, S. Bouwstra, M. Elwenspoek, and J. H. J. Fluitman, J. Vac. Sci. Technol. B **10**, 19 (1992).
[146] E. Majorana and Y. Ogawa, Phys. Lett. A **233**, (1997).
[147] H. J. Butt and M. Jaschke, Nanotechnology **6**, 1 (1995).
[148] A. N. Cleland and M. L. Roukes, J. Appl. Phys. **92**, 2758 (2002).
[149] Z. Djuric, Microelectron. Reliab. **40**, 919 (2000).
[150] K. Y. Yasumura, T. D. Stowe, E. M. Chow, T. Pfafman, T. W. Kenny, B. C. Stipe, and D. Rugar, J. Microelectromech. Syst. **9**, 117 (2000).
[151] H. Kawakatsu, S. Kawai, D. Saya, M. Nagashio, D. Kobayashi, H. Toshiyoshi, and H. Fujita, Rev. Sci. Instrum. **73**, 2317 (2002).
[152] J. E. Bishop and V. K. Kinra, Int. J. Solids Struct. **34**, (1997).
[153] R. A. Buser and N. F. de Rooij, in *IEEE Workshop Micro Electro Mechanical Systems*, Salt Lake City, UT (1989), p. 94.
[154] R. N. Kleiman, G. K. Kaminsky, J. D. Reppy, R. Pindak, and D. J. Bishop, Rev. Sci. Instrum. **56**, 2088 (1985).
[155] R. E. Mihailovich and N. C. MacDonald, Sens. Actuators, A **50**, 199 (1995).
[156] R. E. Mihailovich and J. M. Parpia, Phys. Rev. Lett. **68**, 3052 (1992).

[157] B. H. Houston, D. M. Photiadis, M. H. Marcus, J. A. Bucaro, Xiao Liu, and A. J. F. Vignola, Appl. Phys. Lett. **80**, 1300 (2002).
[158] R. Lifshitz and M. L. Roukes, Phys. Rev. B **61**, 5600 (2000).
[159] R. Lifshitz, Physica B **316**, 397 (2002).
[160] F. P. Milanovich, 1995.
[161] A. Mehta, S. Cherian, and D. H. Thundat, Appl. Phys. Lett. **78**, 1637 (2001).
[162] T. R. Albrecht, P. Grutter, D. Horne, and D. Rugar, J. Appl. Phys. **69**, 668 (1991).
[163] A. K. Deisingh, Analyst (Cambridge, U.K.) **128**, 9 (2003).
[164] R. Maboudian, Surf. Sci. Rep. **30**, 209 (1998).
[165] J. Buhler, E. Fitzer, and D. Kehre, J. Electrochem. Soc. **124**, C299 (1977).
[166] J. Buhler, F. P. Steiner, and H. Baltes, J. Micromech. Microeng. **7**, R1 (1997).
[167] M. Madou, *Fundamentals of Microfabrication* (CRC Press, New York, 1997).
[168] J. W. Gardner, V. K. Varadan, and O. O. Awadelkarim, *Microsensors, MEMS and Smart Devices* (Wiley, New York, 2001).
[169] A. J. Steckl, H. C. Mogul, and S. Mogren, Appl. Phys. Lett. **60**, 1833 (1992).
[170] Y. Zhao, M. Y. Mao, R. Horowitz, A. Majumdar, J. Varesi, P. Norton, and J. Kitching, J. Microelectromech. Syst. **11**, 136 (2002).
[171] C. Hagleitner, A. Hierlemann, D. Lange, A. Kummer, N. Kerness, O. Brand, and H. Baltes, Nature (London) **414**, 293 (2001).
[172] A. Hierlemann, D. Lange, C. Hagleitner, N. Kerness, A. Koll, O. Brand, and H. Baltes, Sens. Actuators B **70**, 2 (2000).
[173] A. Hierlemann, TrAC, Trends Anal. Chem. **21**, IV (2002).
[174] A. Erbe and R. H. Blick, Physica B **272**, 575 (1999).
[175] A. Erbe, C. Weiss, W. Zwerger, and R. H. Blick, Phys. Rev. Lett. **87**, 096106 (2001).
[176] J. L. Corbeil, N. V. Lavrik, S. Rajic, and P. G. Datskos, Appl. Phys. Lett. **81**, 1306 (2002).
[177] N. Abedinov, P. Grabiec, T. Gotszalk, T. Ivanov, J. Voigt, and I. W. Rangelow, J. Vac. Sci. Technol. A **19**, 2884 (2001).
[178] H. L. Tuller and R. Mlcak, J. Electroceram. **4**, 415 (2000).
[179] K. M. Hansen, H. F. Ji, G. H. Wu, R. Datar, R. Cote, A. Majumdar, and T. Thundat, Anal. Chem. **73**, 1567 (2001).
[180] N. V. Lavrik, C. A. Tipple, M. J. Sepaniak, and P. G. Datskos, Proc. SPIE **4560**, 152 (2001).
[181] H. F. Ji, T. Thundat, R. Dabestani, G. M. Brown, P. F. Britt, and P. V. Bonnesen, Anal. Chem. **73**, 1572 (2001).
[182] H. F. Ji, K. M. Hansen, Z. Hu, and T. Thundat, Sens. Actuators B **72**, 233 (2001).
[183] X. H. Xu, T. G. Thundat, G. M. Brown, and H. F. Ji, Anal. Chem. **74**, 3611 (2002).
[184] M. T. Tuominen, R. V. Krotkov, and M. L. Breuer, Phys. Rev. Lett. **83**, 3025 (1999).
[185] D. Rugar, H. J. Mamin, and P. Guethner, Appl. Phys. Lett. **55**, 2588 (1989).
[186] G. Meyer and N. M. Amer, Appl. Phys. Lett. **53**, 1045 (1988).
[187] M. Hoummady, E. Farnault, T. Yahiro, and H. Kawakatsu, J. Vac. Sci. Technol. B **15**, 1539 (1997).
[188] A. Kikukawa, S. Hosaka, Y. Honda, and R. Imura, Jpn. J. Appl. Phys., Part 2 **33**, L1286 (1994).
[189] Y. Hadjar, P. F. Cohadon, C. G. Aminoff, M. Pinard, and A. Heidmann, Europhys. Lett. **47**, 545 (1999).
[190] D. W. Carr, S. Evoy, L. Sekaric, H. G. Craighead, and J. M. Parpia, Appl. Phys. Lett. **75**, 920 (1999).
[191] M. Tortonese, H. Yamada, R. C. Barrett, and C. F. Quate, in *The Proceedings of Transducers '91, IEEE* (Pennington, New Jersey, 1991).
[192] M. Tortonese, R. C. Barrett, and C. F. Quate, Appl. Phys. Lett. **62**, 834 (1996).
[193] J. Thaysen, A. Boisen, O. Hansen, and S. Bouwstra, Sens. Actuators, A **83**, 47 (2000).
[194] Q. M. Wang and L. E. Cross, Ferroelectrics **215**, 187 (1998).
[195] S. Zurn, M. Hseih, G. Smith, D. Markus, M. Zang, G. Hughes, Y. Nam, M. Arik, and D. Polla, Smart Mater. Struct. **10**, 252 (2001).
[196] D. L. DeVoe and A. P. Pisano, J. Microelectromech. Syst. **6**, 266 (1997).
[197] S. S. Lee and R. M. White, Sens. Actuators, A **52**, 41 (1996).
[198] J. H. Lee, K. H. Yoon, and T. S. Kim, Integr. Ferroelectr. **50**, 43 (2002).
[199] J. D. Adams, G. Parrott, C. Bauer, T. Sant, L. Manning, M. Jones, B. Rogers, D. L. McCorkle, and T. L. Ferrell, Appl. Phys. Lett. **83**, 3428 (2003).
[200] R. Amantea, C. M. Knoedler, F. P. Pantuso, V. K. Patel, D. J. Sauer, and J. R. Tower, in *SPIE* (Orlando, FL, 1997), Vol. 3061, p. 210.
[201] L. K. Baxter, *Capactive Sensors, Design and Applications* (IEEE Press, New York, 1997).
[202] T. W. Kenny, W. J. Kaiser, J. A. Podosek, H. K. Rockstad, J. K. Reynolds, and E. C. Vote, J. Vac. Sci. Technol. A **11**, 797 (1993).
[203] G. Binnig and H. Rohrer, IBM J. Res. Dev. **30**, 355 (1986).
[204] T. W. Kenny, W. J. Kaiser, S. B. Waltman, and J. K. Reynolds, Appl. Phys. Lett. **59**, 1820 (1991).
[205] D. DiLella, L. J. Whitman, R. J. Colton, T. W. Kenny, W. J. Kaiser, E. C. Vote, J. A. Podosek, and L. M. Miller, Sens. Actuators, A **86**, 8 (2000).
[206] J. Zhang and S. O'Shea, Sens. Actuators B **94**, 65 (2003).
[207] H. P. Lang, R. Berger, F. Battiston, J. P. Ramseyer, E. Meyer, C. Andreoli, J. Brugger, P. Vettiger, M. Despont, T. Mezzacasa, L. Scandella, H. J. Guntherodt, C. Gerber, and J. K. Gimzewski, Appl. Phys. A: Mater. Sci. Process. **66**, S61 (1998).
[208] S. A. Savran, A. W. Sparks, J. Sihler, J. Li, W.-C. Wu, D. E. Berlin, T. P. Burg, J. Fritz, M. A. Schmidt, and S. R. Manalis, J. Microelectromech. Syst. **11**, 703 (2002).
[209] P. R. Saulson, Phys. Rev. D **42**, 2437 (1990).
[210] M. Kajima, N. Kusumi, S. Moriwaki, and N. Mio, Phys. Lett. A **264**, 251 (1999).
[211] P. W. Kruse, in *Uncooled Infrared Imaging Arrays and Systems, Semiconductors and Semimetals, 47*, edited by P. W. Kruse and D. D. Skatrud (Academic Press, San Diego, 1997).
[212] T. Thundat and L. Maya, Surf. Sci. **430**, L546 (1999).
[213] H. P. Lang, R. Berger, C. Andreoli, J. Brugger, M. Despont, P. Vettiger, C. Gerber, J. K. Gimzewski, J. P. Ramseyer, E. Meyer, and H. J. Guntherodt, Appl. Phys. Lett. **72**, 383 (1998).
[214] H. P. Lang, M. K. Baller, R. Berger, C. Gerber, J. K. Gimzewski, F. M. Battison, P. Fornaro, J. P. Ramseyer, E. Meyer, and H. J. GŸntherodt, Anal. Chim. Acta **393**, 59 (1999).
[215] H. P. Lang, M. K. Baller, R. Berger, C. Gerber, J. K. Gimzewski, F. M. Battiston, P. Fornaro, J. P. Ramseyer, E. Meyer, and H. J. Guntherodt, Anal. Chim. Acta **393**, 59 (1999).
[216] L. A. Pinnaduwage, V. Boiadjiev, J. E. Hawk, and T. Thundat, Appl. Phys. Lett. **83**, 1471 (2003).
[217] L. A. Pinnaduwage, A. Gehl, D. L. Hedden, G. Muralidharan, T. Thundat, R. T. Lareau, T. Sulchek, L. Manning, B. Rogers, M. Jones, and J. D. Adams, Nature (London) **425**, 474 (2003).
[218] P. G. Datskos, S. Rajic, M. J. Sepaniak, N. Lavrik, C. A. Tipple, L. R. Senesac, and I. Datskou, J. Vac. Sci. Technol. B **19**, 1173 (2001).
[219] E. T. Arakawa, N. V. Lavrik, and P. G. Datskos, Ultramicroscopy **97**, 459 (2003).
[220] E. T. Arakawa, N. V. Lavrik, and P. G. Datskos, Appl. Opt. **42**, 1757 (2003).
[221] H. J. Butt, M. Jaschke, and W. Ducker, Bioelectrochem. Bioenerg. **38**, 191 (1995).
[222] H. F. Ji, E. Finot, R. Dabestani, T. Thundat, G. M. Brown, and P. F. Britt, Chem. Commun. (Cambridge) **6**, 457 (2000).
[223] J. Headrick, N. V. Lavrik, M. J. Sepaniak, and P. G. Datskos, Ultramicroscopy **97**, 417 (2003).
[224] A. Subramanian, P. I. Oden, S. J. Kennel, K. B. Jacobson, R. J. Warmack, T. Thundat, and M. J. Doktycz, Appl. Phys. Lett. **81**, 385 (2002).
[225] D. R. Baselt, G. U. Lee, and R. J. Colton, J. Vac. Sci. Technol. B **14**, 789 (1996).
[226] D. R. Baselt, G. U. Lee, K. M. Hansen, L. A. Chrisey, and R. J. Colton, Proc. IEEE **85**, 672 (1997).
[227] R. Raiteri, G. Nelles, H. J. Butt, W. Knoll, and P. Skladal, Sens. Actuators B **61**, 213 (1999).
[228] R. Raiteri, M. Grattarola, H. J. Butt, and P. Skladal, Sens. Actuators B **79**, 115 (2001).
[229] A. Porwal, M. Narsude, V. R. Rao, and S. Mukherji, IETE Tech. Rev. **19**, 257 (2002).
[230] A. M. Moulin, S. J. O'Shea, R. A. Badley, P. Doyle, and M. E. Welland, Langmuir **15**, 8776 (1999).
[231] G. H. Wu, R. H. Datar, K. M. Hansen, T. Thundat, R. J. Cote, and A. Majumdar, Nat. Biotechnol. **19**, 856 (2001).
[232] G. H. Wu, H. F. Ji, K. Hansen, T. Thundat, R. Datar, R. Cote, M. F. Hagan, A. K. Chakraborty, and A. Majumdar, Proc. Natl. Acad. Sci. U.S.A. **98**, 1560 (2001).
[233] R. Marie, H. Jensenius, J. Thaysen, C. B. Christensen, and A. Boisen, Ultramicroscopy **91**, 29 (2002).

[234] B. Ilic, D. Czaplewski, H. G. Craighead, P. Neuzil, C. Campagnolo, and C. Batt, Appl. Phys. Lett. **77**, 450 (2000).
[235] A. S. Olkhovets, S. Evoy, D. W. Carr, J. M. Parpia, and H. G. Craighead, J. Vac. Sci. Technol. B **18**, 3549 (2000).
[236] Y. T. Yang, K. L. Ekinci, X. M. H. Huang, L. M. Schiavone, and M. L. Roukes, Appl. Phys. Lett. **78**, 162 (2001).
[237] T. B. Gabrielson, IEEE Trans. Electron Devices **40**, 903 (1993).
[238] T. B. Gabrielson, J. Vibr. Acoust. **117**, 405 (1995).
[239] H. P. Lang, M. Hegner, E. Meyer, and C. Gerber, Nanotechnology **13**, R29 (2002).